DEVELOPING SMALL MOLECULE INHIBITORS TARGETING REPLICATION PROTEIN A FOR PLATINUM-BASED COMBINATION THERAPY

Akaash K Mishra

Submitted to the faculty of the University Graduate School
in partial fulfillment of the requirements
for the degree
Master of Science
in the Department of Biochemistry and Molecular Biology,
Indiana University

December 2014

Accepted by the Graduate Faculty, Indiana University, in partial fulfillment of the requirements for the degree of Master of Science.

Master's Thesis Committee

John J. Turchi, Ph.D., Chair

Mark R. Kelley, Ph.D.

Thomas D. Hurley, Ph.D.

Zhong-Yin Zhang, Ph.D.

Acknowledgements

I would like to express my deep and sincere gratitude to my supervisor, Dr. John Turchi. I am grateful to him for having me in his lab, showing faith and confidence in me and training me for my scientific endeavour. His wide knowledge and his logical way of thinking have been of great value for me. His understanding, encouragement and personal guidance have provided a good basis for the present thesis.

I am thankful to my committee members – Dr. Mark Kelley, Dr. Thomas Hurley and Dr. Zhong-Yin Zhang for their detailed and constructive comments, and for their critical support throughout this work.

Cheers to the past and present Turchi Lab members for making me experience a wonderful time in the lab. I would like to specifically thank Dr. Silvana Dormi for her contribution with her organic chemistry skills and for helping me learn chemical synthesis and NMR. I thank Dr. Derek Woods for his contribution in the *in vivo* work and Pamela VanderVere-Carozza for helping me with cell culture and managing all lab requirements so well. I am indebted to Dr. Jennifer Earley for her purified protein preparations of RPA and RPA-A/B Box and Alaina Turchi for performing the fluorescent displacement assays. I owe my special thanks to all Turchi lab members for their able guidance throughout my project.

A special thanks to Dr. Lawrence Einhorn and the IU Simon Cancer Center (Lung and Testicular Cancer Research Program) for funding and support, Dr. Karen Pollok for support with the *in vivo* core and Dr. Zhong-Yin Zhang for access to the Chemical Genomics Core Facility and equipment support.

I wish to express my warm and sincere thanks to Dr. Shadia Jalal and Dr. Catherine Sears for bestowing their loving attitude towards me and guiding me whenever required.

A special appreciation for Robin Dewalt and Dr. Cecilia Devlin who helped me by generously sharing the lab supplies and guiding me with their expertise when needed.

I owe my loving thanks to my family and my friends. Without their encouragement and understanding it would have been impossible for me to finish this work.

Akaash K Mishra

DEVELOPING SMALL MOLECULE INHIBITORS TARGETING REPLICATION PROTEIN A FOR PLATINUM BASED COMBINATION THERAPY

All platinum (Pt)-based chemotherapeutics exert their efficacy primarily via the formation of DNA adducts which interfere with DNA replication, transcription and cell division and ultimately induce cell death. Repair and tolerance of Pt-DNA lesions by nucleotide excision repair and homologous recombination (HR) can substantially reduce the effectiveness of the Pt therapy. Inhibition of these repair pathways, therefore, holds the potential to sensitize cancer cells to Pt treatment and increase clinical efficacy. Replication Protein A (RPA) plays essential roles in both NER and HR, along with its role in DNA replication and DNA damage checkpoint activation. Each of these functions requires RPA binding to single-stranded DNA (ssDNA). We synthesized structural analogs of our previously reported RPA inhibitor TDRL-505, determined the structure activity relationships and evaluated their efficacy in tissue culture models of epithelial ovarian cancer (EOC) and non-small cell lung cancer (NSCLC). These data led us to the identification of TDRL-551, which exhibited a greater than 2-fold increase in *in vitro* and cellular activity. TDRL-551 showed synergy with Pt in tissue culture models of EOC and in vivo efficacy, as a single agent and in combination with platinum, in a NSCLC xenograft model. These data demonstrate the utility of RPA inhibition in EOC and NSCLC and the potential in developing novel anticancer therapeutics that target RPA-DNA interactions.

John J. Turchi, Ph.D., Chair

Table of Contents

List of Tables

List of Figures

List of Abbreviations

ABC	ATP-binding cassette
ATM	ataxia telangiectasia mutated
ATR	ataxia telangiectasia and Rad3 related
BRCA1	breast cancer type 1
BRCA2	breast cancer type 2
Cisplatin	cis-diamminedichloroplatinum-(II)
CTR1	copper transporter protein 1
DBD	DNA binding domain
DSB	double strand break
EMSA	electrophoretic mobility shift assay
EOC	epithelial ovarian cancer
ERCC1	excision repair cross-complementation group 1
FBS	fetal bovine serum
GSH	reduced glutathione
HMG	high mobility group
HR	homologous recombination
ICR	Inter-strand crosslink repair
MAPK	mitogen-activated protein kinases
MMR	mismatch repair
NER	nucleotide excision repair
NOD	non-obese diabetic
NSCLC	non-small cell lung cancer

OB	oligonucleotide binding
OS	overall survival
PFS	progression free survival
Pt	platinum
Rad51	Rad51 recombinase
RPA	replication protein A
RPA-A/B	DBD A and B of RPA protein
RPAi	RPA inhibitor
RPMI	Roswell park memorial institute medium
SCID	severe combined immunodeficiency
SMI	small molecule inhibitor
SSB	single stranded DNA binding protein
ssDNA	single stranded DNA
TDRL	Turchi DNA repair laboratory
TFIIH	transcription factor II human
XPA	xeroderma pigmentosum group A
XPF	xeroderma pigmentosum group F
XPG	xeroderma pigmentosum group G

1. INTRODUCTION

1.1. Platinum based chemotherapy – a major landmark in the history of anticancer treatment regimens.

Platinum (Pt) was the first metal to be established as a cancer chemotherapeutic (1). Cisplatin, the first Pt-based drug continues to be the most commonly prescribed agent for cancer treatment half a century since the serendipitous discovery of its biological properties (2). The use of cisplatin has had a major impact especially in the treatment of solid malignancies such as testicular, ovarian and lung cancer. Particularly in the case of testicular cancer, platinum in combination with other chemotherapeutic agents –bleomycin and etoposide remarkably improved the survival rates in patients from 5% to upto 95% (3). This was a major landmark in the history of successful anticancer drugs.

Although highly efficacious, some of the major concerns with cisplatin-based therapy were its side effects particularly nephrotoxicity and neurotoxicity, which led to the development of its structural analogue carboplatin (4). Carboplatin has similar efficacy to cisplatin with reduced side effects. The mechanism of action for cisplatin and carboplatin involves coordinate covalent binding to the purine bases of DNA (4). Cisplatin (chemical formula: *cis*-$[Pt(Cl)_2(NH_3)_2](II)$) (becomes activated by an intra-cellular process of aquation and displacement of one of its chloride leaving groups. This form of cisplatin actively reacts to one of the purine bases, preferably guanine and forms a coordinate covalent bond. Subsequently, the other chloride group in cisplatin also gets displaced resulting in Pt-DNA crosslinks. 1,2-intrastrand crosslinks (that are produced when Pt reacts with two adjacent guanines) are more

common than the 1,3-intrastrand crosslinks (that result from the reaction of Pt with two non adjacent guanines with one nucleotide base in between). Interstrand crosslinks are rare and constitute less than 5% of Pt-DNA lesions. Pt-DNA adducts interfere with DNA replication, transcription and cell division and ultimately induce apoptotic cell death.

1.2. Platinum Resistance in Epithelial Ovarian Cancer

Resistance to Pt-based chemotherapeutic agents has been a major limitation for successful treatment for a wide variety of cancers. Epithelial ovarian cancer (EOC) is one of the most sensitive solid tumors to Pt-based chemotherapy. However more than 80% of the patients relapse with Pt-resistant disease, where second line therapies are largely ineffective (5). Thus, clinicians have designated ovarian cancer as the most deadly gynecological cancer. In the past decade, there has been no significant improvement in the cure rate of ovarian cancer. Overall survival (6) of the patients has increased marginally due to better patient care and increase in choice for second line therapies, nonetheless progression free survival (PFS) still remains the same (7). The combination of carboplatin and paclitaxel continues to be the standard first line therapy for the treatment of EOC. Although a large number of second line therapies are available for patients relapsing with Pt-resistant cancers, most of them have been effective only in small subsets of the patient population. There is a need to systematically evaluate many of these novel drugs as single agents or in combination with chemotherapy. The second line treatment options following recurrence are subdivided into two categories: 1) retreatment with cisplatin or carboplatin for Pt sensitive recurrence (patients relapsing after 6

months post Pt-based chemotherapy) 2) Non Pt-based drug therapy for Pt-refractory or Pt-resistant recurrence (patients relapsing during or less than 6 months post Pt-based chemotherapy) (8). A number of drugs such as paclitaxel, doxorubicin, gemcitabine and bevacizumab have been used in trials as second line therapies for Pt-resistant EOC with response rates from 10-35% (9).

1.3. Platinum Resistance in Non-Small Cell Lung Cancer

Non-small cell lung cancers (NSCLCs) are often intrinsically insensitive to chemotherapy (10). Moreover majority of the patients are diagnosed post metastasis making it difficult to use other treatment options such as surgery and radiation. However, whenever possible surgery is increasingly being combined with both pre-operative (neo-adjuvant chemotherapy) and post-operative (adjuvant chemotherapy) chemotherapy involving cisplatin. The 5-year rate of OS in non-small cell lung cancer (NSCLC) still remains below 15% (10). The most common types of NSCLCs can be categorized into three types – adenocarcinoma (most common type of lung cancer and most typical in non smokers) and, squamous cell carcinoma (more common in men and correlated to smoking history) and large cell carcinoma (heterogeneous and less than 10% of NSCLC) (6,11,12). A number of targeted therapies have been developed in the past for the treatment of lung cancers with specific genetic mutations. For example, drugs crizotinib and ceritinib targeting the ALK gene re-arrangement. Other prominent drugs are the tyrosine kinase inhibitors such as gefitinib and erlotinib and angiogenesis inhibitor bevacizumab (13). Each of these has had minimal to moderate success depending on the target population (14). Moreover tumors that are resistant to one type of drug are often

seen to be resistant to other drugs as well or in some cases acquire resistance over time to other drugs. Although numerous mechanisms have been delineated for drug resistance in lung cancer we are still far away from establishing effective strategies to overcome drug resistance. Thus, extensive targeting of underlying drug resistance mechanisms becomes utmost important.

1.4. Cisplatin – mechanism of action

An understanding of the mode of action of cisplatin is cardinal for elucidating the different mechanisms leading to cisplatin resistance. As briefly mentioned earlier, cisplatin by itself is an inert molecule and it must be activated by a series of aquation reactions inside the cell. The aquation reactions involve the substitution of the chloride groups (one or both) with water molecules within the cell. The relatively low concentration of chloride ions inside the cytoplasm (~2-10 mM as compared to 100 mM in extracellular milieu) facilitates this reaction to take place spontaneously generating mono and bi-aquated forms of cisplatin that are highly reactive (4). However it's interesting to note that only 1% of the intra-cellular cisplatin actually hits its primary target – the nuclear DNA. The rest of the activated cisplatin molecules are subjected to a wide variety of cytoplasmic substrates, especially endogenous nucleophiles such as reduced glutathione (GSH) and other proteins with cysteine residues. This also has the potential to shift the redox balance inside the cell towards oxidative stress that can further facilitate DNA damage (15). Aquated cisplatin covalently binds DNA with a propensity for N7-sites on purine bases and generates protein-DNA complexes and intra- and inter-strand DNA adducts (Figure 1). Guanine bases are preferred over adenine for the formation of

coordinate covalent bonds. 95% of the Pt-DNA adducts constitute of intrastrand adducts, while interstrand adducts account for less than 5% (Figure 1). It's noteworthy to point out that the active form of carboplatin, a cisplatin analogue, is identical to cisplatin and forms exactly the same type of DNA lesions (4).

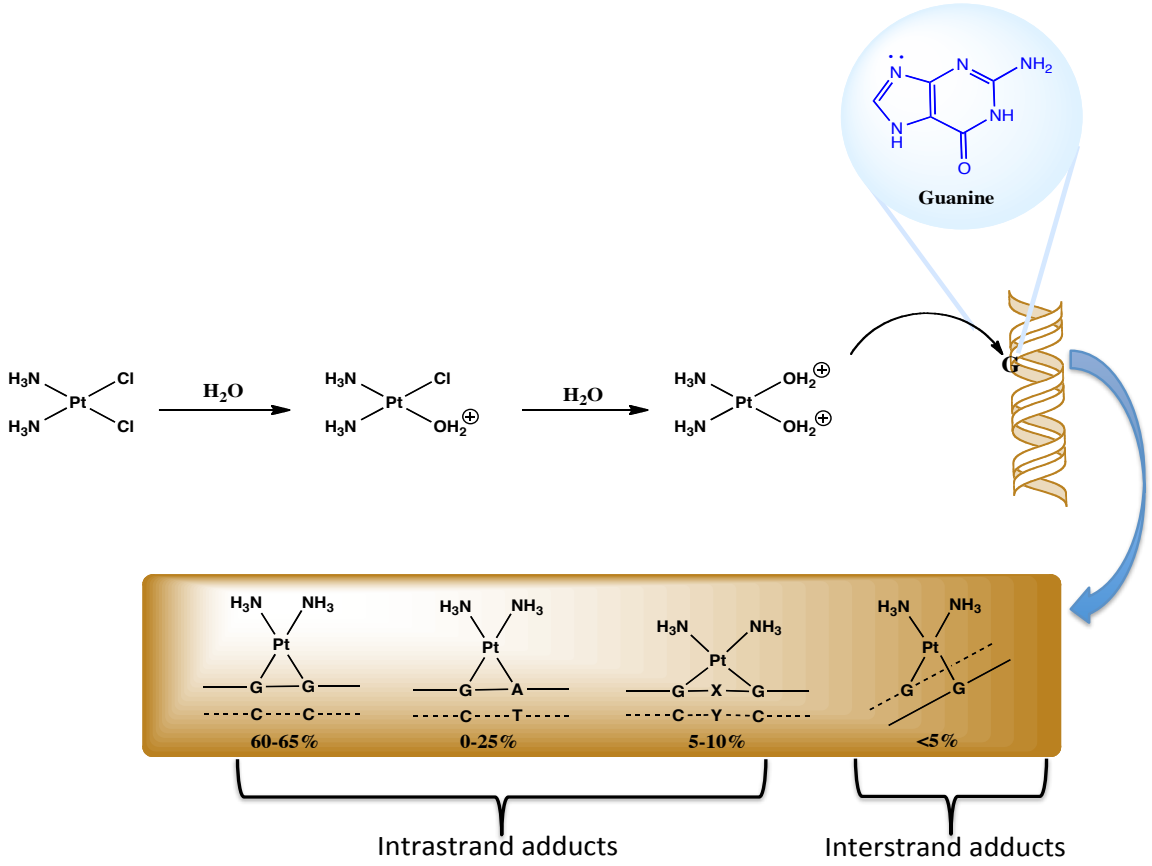

Figure 1: Intracellular activation of cisplatin to form Pt-DNA adducts. The solid and dotted black lines on the bottom part of the figure represent the two strands of DNA. A, G, C, T represent the nucleotide bases adenine, guanine, cytosine and thymine respectively. X and Y represent a complementary pair of nucleotide bases.

Although the exact mechanism for cisplatin cytotoxicity is still elusive, DNA-damage and mitochondrial apoptosis is the most well established mode of action for

cisplatin (Figure 2) (16-18). Multiple repair pathways including nucleotide excision repair (NER), homologous recombination (HR) (including the fanconi anemia proteins) and mismatch repair (MMR) recognize cisplatin induced DNA lesions (5). The balance between DNA damage and DNA repair dictates tumor cell death (Figure 2). If the extent of DNA damage is limited then the damage induced S and G2 phase cell cycle arrest play a protective role by allowing time for repair and preventing aberrant mitosis. However if the extent of DNA damage is beyond repair the cells are programmed for apoptotic cell death. Current theories also implicate cell specific differences in repair versus apoptosis balance (19). The major signaling mechanism that translates cisplatin induced DNA damage to apoptosis involves the activation of the DNA damage regulators namely ataxia telangiectasia mutated (ATM) and RAD3-related protein (ATR) (20), checkpoint kinases CHK1 and CHK2 and phosphorylation and stabilization of p53 (Figure 2) (4). p53 activation signals mitochondrial permibilization by release of apoptogenic factors or increased death receptor signaling which ultimately lead to caspase activation and cell death. This process is further facilitated by binding of damage recognition proteins that bind to physical distortions in DNA induced by intrastrand Pt-DNA adducts. Such proteins include components of MMR, the high mobility group of proteins (HMG), the human RNA polymerase I transcription 'upstream binding factor' (hUBF), and the transcription factor 'TATA binding protein' (TBP) (13). Cisplatin has also been shown to activate the mitogen-activated kinase (MAPK) system pathways, however the relative contribution of these pathways to cisplatin cytotoxicity is unclear.

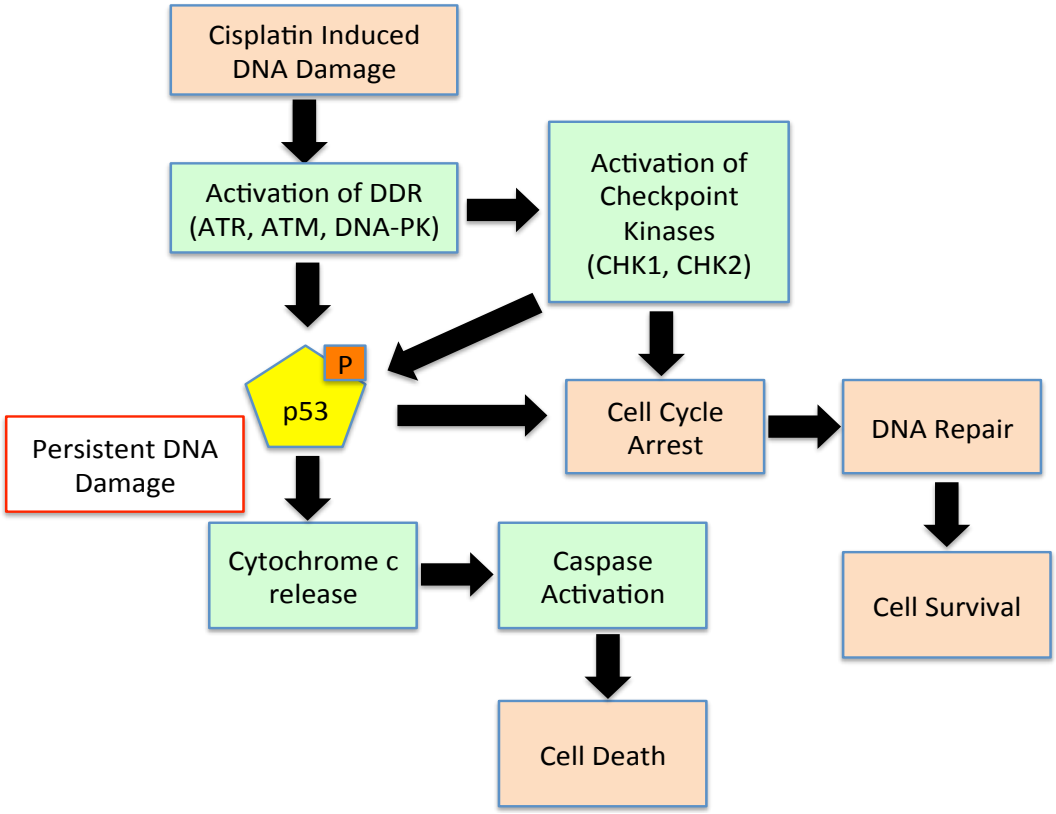

Figure 2: Balance between DNA damage and DNA repair dictates tumor cell death.

1.5. Major Contributors for Platinum Resistance

Chemoresistance is still the major factor that radically limits the clinical utility of cisplatin as an anticancer drug. The major contributors for platinum resistance have been categorized into four groups (Figure 3) – 1) factors that act prior to the drug-target interaction (pre-target factors), 2) factors that act at the site of drug-target interaction (on-target factors), 3) factors that act post drug-target interaction (post-target factors) and 4) factors independent of drug-target interaction (off-target factors) (4).

The pre-target factors include reduced uptake of the drug, increased efflux of the drug and inactivation of the drug before it hits its target. Earlier thought to be

via passive diffusion, the mode of transport for cisplatin into the cells has been linked to the copper transporter CTR1 (21). A decrease in CTR1 expression on the plasma membrane can reduce the intracellular uptake of cisplatin and hence contribute to platinum resistance. Similarly overexpression of ABC (ATP-binding cassette) transporters (ex: MRP2 (multidrug resistance protein-2) and ATP7A (p-type ATPase)) that actively efflux cisplatin out of the cells may lead to platinum resistant cancers (22,23). Furthermore, increased cytoplasmic inactivation of cisplatin (after the aquation reaction) by nucleophilic scavengers such as GSH, methionine, metalothioneins and other cysteine rich proteins may drastically limit the active concentration of cisplatin within the cells, thus causing chemoresistance (15).

The on-target factors primarily include an altered capacity of repair and tolerance of the Pt-DNA adducts. A series of DNA repair pathways have been linked to Pt-resistance. NER is the major pathway for the removal of Pt-DNA lesions (primarily intra-strand crosslinks) and NER efficiency in many cancers has been directly correlated to platinum resistance (24,25). Conversely defects in this pathway have been linked to the platinum sensitivity in cancer cells (26). Proteins of the MMR pathway have been shown to recognize Pt-DNA lesions but fail to repair such adducts and hence may signal a pro-apoptotic cascade (27). Hence some Pt-resistant cancers are associated with the deficiency of MMR proteins such as MSH2 and MLH1, since the futile cycle of MMR contributes to killing mechanisms. Translesion synthesis, also known as replicative bypass is another mechanism that contributes to platinum resistance by tolerance of Pt-DNA lesions (28). The DNA-

synthesis in this case is not stalled at the site of the DNA lesion, but instead just proceeds beyond the Pt-adducts. The inter-strand Pt-DNA crosslinks are recognized by a group of fanconi anemia proteins that constitute the inter-strand crosslink repair (ICR) pathway (29). Such crosslinks often result in a double strand break (DSB) and are further repaired by the HR pathway during the S-phase of the cell cycle. HR also plays a crucial role in tolerance of both intra-strand and inter-strand Pt-DNA adducts. Both ICR and HR status have been shown to correspond to cisplatin sensitivity and resistance (20,30,31).

The post target platinum resistance can be due to a defect in signal transduction of the apoptotic cascade or due to a defect in the cell death machinery itself. p53 status has been observed to be a powerful determinant of platinum sensitivity in a wide variety of cancers (32). Overexpression of anti-apoptotic proteins such as BCL-2, BCL-X_L and MCL-1 has been shown to confer resistance to Pt (33-36).

Finally, off-target factors could contribute to the cisplatin resistant phenotype by alteration in signaling of pathways independent to cisplatin that however compensate for the cisplatin induced effects. For example, ERBB2/HER-2 overexpression and PI3K/AKT1 activation has been linked to Pt-resistance in NSCLC patients by promoting cell cycle arrest and allowing more time for repair of Pt-DNA adducts (4). Dual-specificity Y-phosphorylation regulated kinase 1B (DYRK1B) is overexpressed in solid tumors and its depletion sensitizes NSCLC and ovarian cancer cells to cisplatin due to increased oxidative stress (37). Deficiency in the pro-apoptotic MAPK signaling has also been associated with cisplatin resistance,

however no correlation exists between expression levels of MAPK family members and Pt-sensitivity.

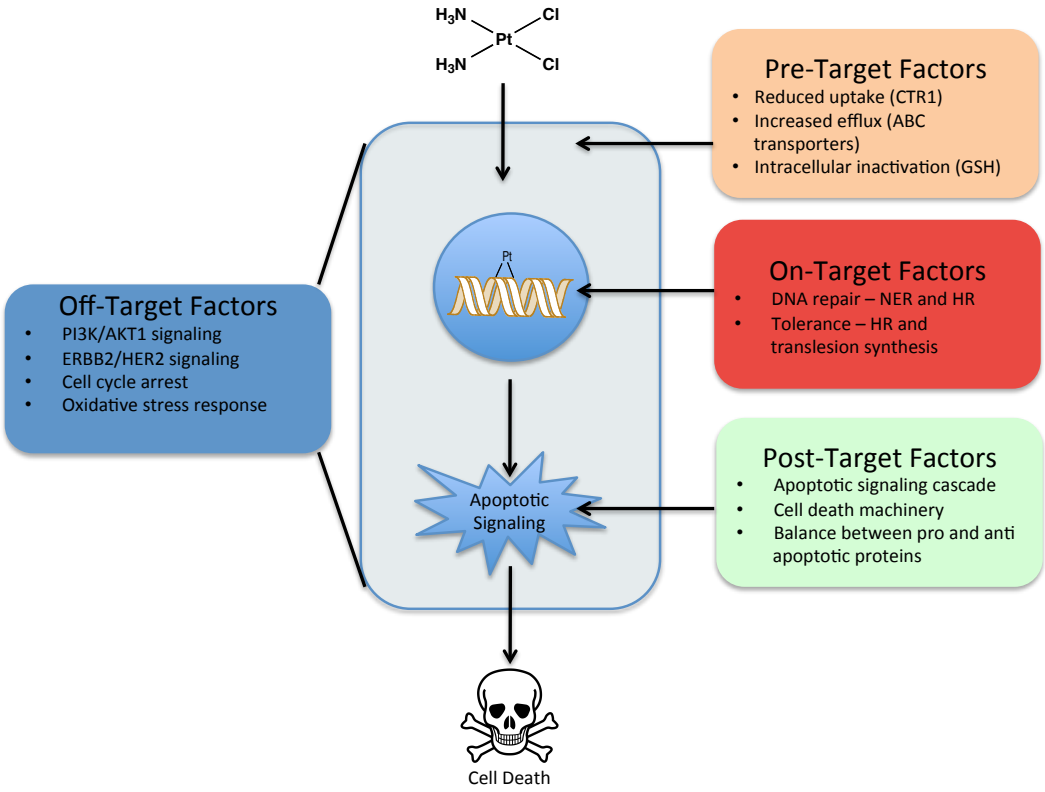

Figure 3: Major contributing factors for platinum resistance. The rectangular region represents a cancer cell and the sphere inside represents the nucleus of the cell. The major contributors for platinum resistance have been categorized based on their relation to Pt-DNA interaction.

1.6. NER and HR in Pt Resistance

NER being the principal pathway for the removal of Pt-DNA adducts plays a critical role in the Pt-sensitivity/resistance of cancer cells. Its importance is highlighted by the fact that testicular cancer cells are hypersensitive to Pt-treatment due to an underlying cellular defect in this pathway (26). Restoration of NER activity re-establishes the Pt-sensitivity back to normal levels. An increase in the expression

of NER component excision repair cross-complementing 1 (ERCC1) or ERCC1-XPF has been associated with Pt-resistance in NSCLC (24). Xeroderma pigmentosum A (XPA), another critical NER factor, was overexpressed in cisplatin resistant ovarian cancers and contributed to increased NER activity (38).

HR is the other major pathway for both repair and tolerance of Pt-DNA lesions. HR genes BRCA1 and BRCA2 are often mutated in a large number of breast and ovarian cancers. It's well established that HR deficient cancers are more sensitive to cisplatin as compared to their HR proficient counterparts. For example, BRCA deficient cancers are generally more responsive to cisplatin and have a better prognosis (30). Conversely up-regulation of BRCA1 has been associated with repair-mediated resistance to cisplatin (32). Furthermore, it has been shown that resistance can be acquired in certain BRCA deficient cancers that are initially sensitive to Pt treatment by certain accompanying mutations accumulated over time that restore the HR function by compensating for the BRCA deficiency (39,40). Taken together, HR status serves an independent marker of cisplatin sensitivity.

1.7. RPA and its role in NER and HR

RPA is the major human ssDNA binding protein and is required for both NER and HRR (41). The RPA heterotrimer consists of 70 kDa, 32 kDa and 14 kDa subunits (Figure 4) with the 70-kDa subunit containing the two major high affinity DNA binding domains (DBD) DBD A and B, as well as DBD C and F. DBD D and E are in the 32-kDa and 14-kDa subunit, respectively. Binding to short stretches of ssDNA (~ 8-10 nucleotides (nts)) is primarily mediated by DBD A and B, while intermediate length ssDNA (~ 12-23 nts) also involves DBD C. Longer length ssDNA

(~ 28-30 nts) engages DBD D in addition to DBDs A, B and C (42-44). Recent reports however contest the conventional 3 distinct modes of binding for RPA. Crystal structure and x-ray scattering studies suggest that RPA binding to ssDNA is stable in only two modes – the low affinity binding mode (8-10 nts involving DBD A and B) and the high affinity binding mode (28-30 nts involving DBD A, B, C and D) (45,46). Besides the RPA-protein interactions are compatible only with the low affinity binding mode.

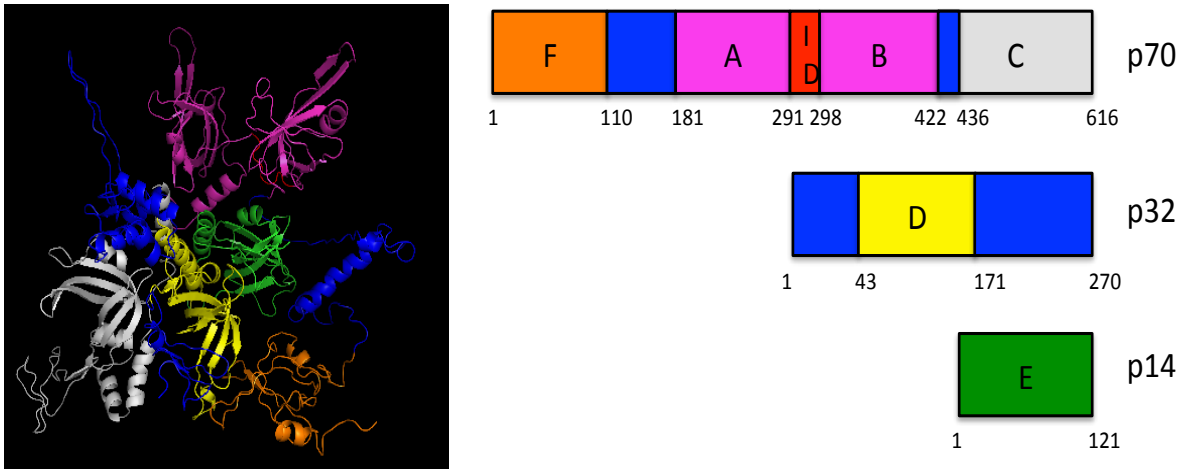

Figure 4: Structure of RPA with oligonucleotide binding (OB) domains. On the left is shown the protein structure of RPA as modeled by Dr. Gerald Alter and group (47). The PDB file of the structure was analyzed and color schemed by PYMOL software. On the right is a schematic representation of the 3 peptide chains that constitute the RPA heterotrimer with the OB folds (A-F) and the inter-domain (ID) region color matched with the structure on the left. The numbers represent the amino acid positions for each domain.

RPA plays essential and non-redundant roles in both NER and HR, apart from its role in replication and DNA damage checkpoint activation. Each of these roles requires binding of RPA to ssDNA, making RPA-DNA interactions a promising target for anti-cancer therapeutic activity in combination with cisplatin (Figure 5). RPA plays a critical role in the initial phase of HR by binding to ssDNA and preventing it to form secondary structures by self-complementation or getting degraded by endonucleases (48). RPA bound ssDNA acts as a substrate for the formation of a nucleoprotein filament by Rad51 and its cofactors, which further drives the process of HR mediated DNA repair (Figure 5) (49). Moreover depletion of RPA protein inhibits RAD51 foci formation and repair of double stranded breaks through HR (50). During NER, RPA binds ssDNA in the opened DNA complex (resulting from helical distortion by the intra-strand DNA lesion or opening up of the damaged DNA bubble by TFIIH helicase activity) and helps in stabilization of the repair complex at the site of DNA damage (Figure 5) (51). RPA bound to ssDNA also interacts with other NER proteins like XPA, XPG and XPF and helps in recruitment and proper positioning of the endonucleases (XPG and ERCCI-XPF) that are responsible for the dual incisions around the DNA lesion. Additionally RPA not only acts during the pre-incision steps but also remains bound to the ssDNA post excision and facilitates the gap-filling repair synthesis by DNA polymerases. Furthermore *in vitro* reconstituted NER demonstrates RPA as absolutely essential for repair of Pt-DNA adducts (52). Clearly RPA's role is absolutely critical in both the DNA repair processes –HR and NER.

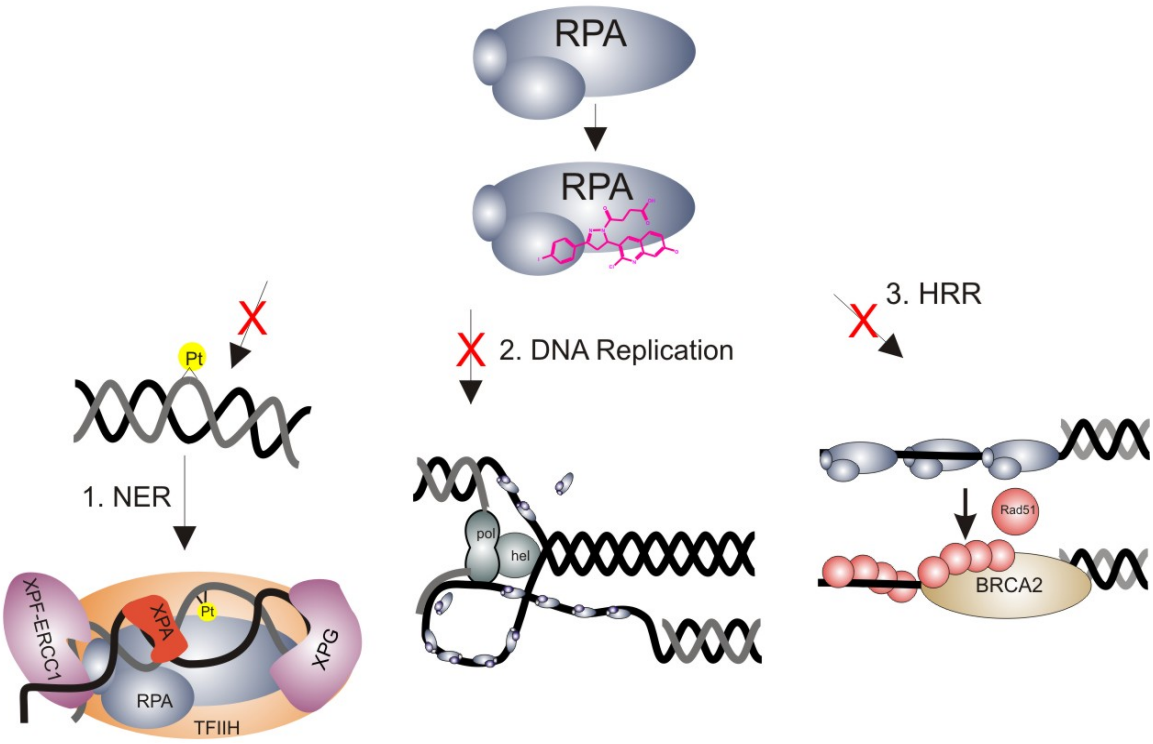

Figure 5: Role of RPA in NER, HRR and DNA replication. HRR indicates homologous recombination and repair.

1.8. Chemical Synthetic Lethality in Conjunction with DNA Damage

Structural analysis of RPA reveals unique protein-DNA interactions that would facilitate the design of potent and selective small molecule inhibitors (SMIs) (46). It has been also shown that genetic mutants of RPA with defects in DNA repair function do not impact DNA replication and similarly some replication defective RPA mutants display DNA repair proficiency (41,53,54). This separation of function can be exploited by using chemical probes that exclusively interfere with the DNA repair pathway and that, in conjunction with DNA-damaging agents, would offer a new possibility for cancer treatment. Our group has previously reported both reversible and irreversible chemical inhibitors of RPA (55-58). The reversible

inhibitor TDRL-505 exhibits synergistic effects with DNA damaging agents in a lung cancer cell model. This small molecule hinders the binding of DBD A and B of RPA to ssDNA, which according to *in silico* docking analysis occurs as a consequence of its interaction with DBD B and the DBD A-B interdomain (58). Therefore, for the present study, we screened TDRL-505 along with a series of analogs and evaluated their activity in an EOC cell culture model. SAR data led us to an optimized lead compound, TDRL-551. Herein we report the *in vitro,* cellular and *in vivo* activity of TDRL-551 in models of lung and ovarian cancer. Our model (Figure 6) represents an artificial system of synthetic lethality with our inhibitors impairing a critical protein function that is synergistically lethal in combination with DNA damaging agents. Since RPA inhibition disrupts both NER and HR – the major pathways for Pt-DNA repair, its combination therapy with platinum has immense potential for the treatment of a wide variety of cancers.

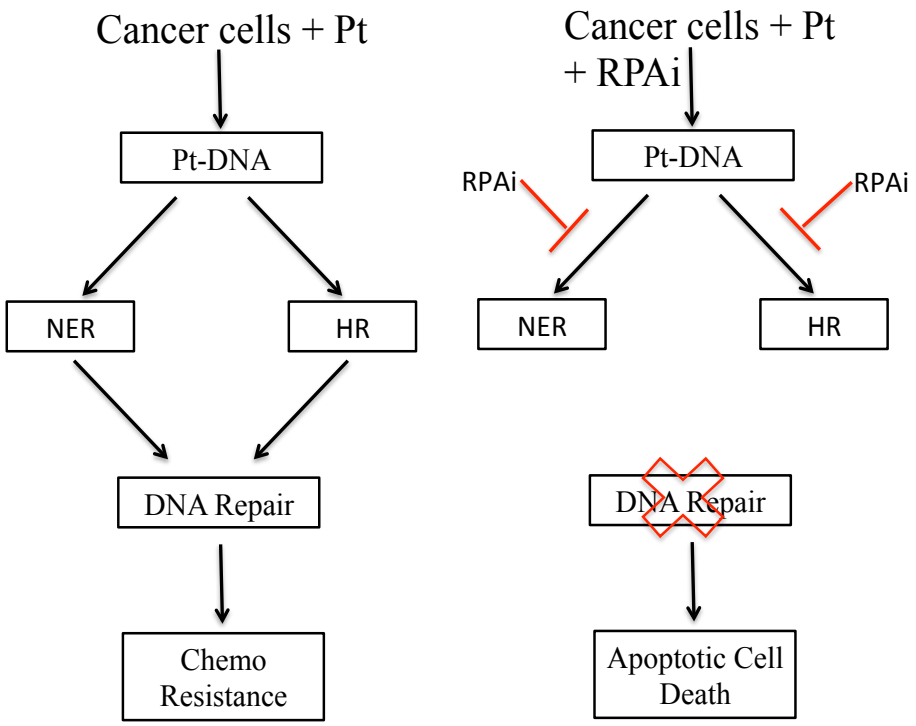

Figure 6: Model for synthetic lethality with RPA inhibitors (RPAi) and platinum (Pt).

2. MATERIALS AND METHODS

2.1. Electrophoretic Mobility Shift Assays (EMSA)

2.1.1. *General*

Human RPA was expressed in *E. coli* and purified by affinity purification as previously described (40). 20 μL EMSA reactions were performed with 50 nM RPA and 2.5 nM 5'[^{32}P]-labeled 34-base DNA in buffer containing 20mM HEPES (pH 7.0), 1mM DTT, 0.001% NP-40, 100 mM NaCl, 5 mM $MgCl_2$ and 50 μg/ml bovine serum albumin. Chemical compounds, either purchased from ChemDiv or synthesized in our laboratory, were suspended in DMSO and titrated as detailed in each figure. The DMSO concentration in the reaction mixture was kept constant at 5% or below. RPA in the reaction buffer was incubated with inhibitor/DMSO for 30 minutes before the addition of DNA. This was followed by 5 minutes of post DNA incubation for RPA-DNA binding. Reactions were carried out at room temperature and 6% native polyacrylamide gels were used to separate the products. The bound and unbound fractions were then quantified by phosphor-imager analysis using the ImageQuant software (Molecular Dynamics, CA).

2.1.2. DNA Radiolabeling

The DNA radiolabelling reaction mixture contained 10 pmols of 34-base DNA, 20 pmols of γ-P^{32} ATP, 1X T4 PNK Buffer and 10 units of T4 PNK. Water was added to make up the reaction volume to 50 μl. The above reaction mixture was incubated at 37°C for 30 mins. In order to ensure that the DNA was uniformly phosphorylated, 1 ul of ATP (1mM) was added to the 50 ul reaction and incubate for 5 min at 37°C. 4 ul of EDTA was added to stop the reaction and incubated at 70°C for

5 mins. The total reaction volume became 55 ul. So we had 10 pmol of DNA in 55 ul reaction. 1 ul of reaction was diluted 1:10 and 1 ul of this dilution was taken and spotted on DE81 filter paper and dried. The spotted filter paper was washed 3x with 0.5M PO_4 pH 7.0 (~10ml), dried and counted in scintillation counter with scintillation fluid. The specific activity for the kinase reaction was calculated as follows:

Specific activity = (CPM1*dilution*total reaction volume)/total pmols of DNA = CPM/pmol DNA

G-50 columns were made with glass beads on bottom of 0.5 ml tubes with hole in it. The rest of the tubes were filled with G50 matrix. The tubes were centrifuged for 5 mins at 1000g. The best column was selected out of a sample of 4-6 on visual inspection for cracks in the column.

All remaining 54 ul of the remaining DNA labeling reaction mix was added to the selected minicolumn. This column was then centrifuged for 5 mins at 1000 g. 1 ul of purified DNA was diluted 1:10 and 1 ul of this dilution was taken and spotted on DE81 filter paper. The filter paper was dried and counted on scintillation counter with scintillation fluid. The DNA concentration was determined as follows:

DNA Concentration = CPM2*10/Specific Activity.

2.1.3. *EMSA with RPA-A/B Box*

The RPA-A/B construct was expressed as a SUMO-His_6-$RPA^{181-432}$ fusion protein. E. coli BL21 (DE3) cells in log growth were induced for 3 hours with 0.5mM IPTG at 37°C. The cells were lysed in buffer containing 50mM Tris pH 7.5, 300 mM NaCl, 10% sucrose, 10mM imidazole, 25 µg/ml lysozyme, 1 µg/ml leupeptin, 1

μg/ml pepstatin and 0.5 mM PMSF. The lysate was loaded onto a Ni-NTA column washed and then incubated overnight with wash buffer containing 3 μg/ml ULP1 protease to cleave the SUMO tag. The cleaved His_6-$RPA^{181-432}$ was eluted from the Ni-NTA column with elution buffer containing 350 mM imidazole. The His6-RPA was then further purified on a size exclusion column to remove the cleaved SUMO tag fragment. The elute pool from the size exclusion column was then concentrated and stored at -80°C. The EMSA reactions contained 125 nM RPA-A/B Box in 20 ul reactions and the gel was pre-chilled and ran at 4° C. The rest of the reaction conditions were identical to as described above in the general section.

2.2. Chemical Synthesis

2.2.1. *General*

All solvents and chemicals were used as purchased from commercial suppliers. ^{1}H NMR spectra were obtained on a Bruker Avance III 500 MHz NMR spectrometer. Chemical shifts are expressed in parts per million (ppm, d), relative to tetramethylsilane (TMS) as internal reference. Signals are described as *s* (singlet), *d* (doublet), *dd* (doublet of doublets), *dt* (doubles of triplets), *t* (triplet), *q* (quartet), or *p* (pentet).

2.2.2. 2-chloro-7-ethoxy-3-(3-(4-iodophenyl)-4,5-dihydro-1H-pyrazol-5-yl)quinoline (7a, Figure 5)

NaOH (0.83 mL, 2.5 M in water, 2.07 mmol) was added dropwise to a solution of 4-iodoacetophenone (0.36 g, 1.47 mmol) and 2-chloro-7-ethoxyquinoline-3-carbaldehyde (0.35 g, 1.47 mmol) in EtOH (12 mL). After stirring for a 45 min at 40 °C, the reaction mixture was quenched with HCl (1.38 mL, 3 M).

The crude mixture containing the resulting enone was then filtered, thoroughly washed with EtOH, and used in the next step without further purification. Hydrazine monohydrate (0.36 mL, 7.33 mmol) was added dropwise to a suspension of the enone obtained in the previous step in EtOH (30 mL). The mixture was refluxed for 1.5 h with stirring, after which it was allowed to cool to room temperature. The obtained solid was filtered and washed with EtOH. Further purification by trituration with EtOH furnished the title compound as an off-white solid (0.57 g, 81% over 2 steps). ^{1}H NMR (500 MHz, DMSO-d_6) d 1.41 (*t*, J=7.0 Hz, 3H), 2.89 (*dd*, J=16.5, 10.0 Hz, 1H), 3.67 (*dd*, J=16.5, 11.0 Hz, 1H), 4.20 (*q*, J=7.0 Hz, 2H), 5.19 (*dt*, J=10.5, 3.5 Hz, 1H), 7.27 (*dd*, J=9.0, 2.5 Hz, 1H), 7.34 (*d*, J=2.5 Hz, 1H), 7.44 (*d*, J=8.5 Hz, 2H), 7.74 (*d*, J=8.5 Hz, 2H), 7.84 (*d*, J=3.5 Hz, 1H), 7.97 (*d*, J=9.0 Hz, 1H), 8.42 (*s*, 1H).

2.2.3. 4-(5-(2-chloro-7-ethoxyquinolin-3-yl)-3-(4-iodophenyl)-4,5-dihydro-1H-pyrazol-1-yl)-4-oxobutanoic acid (9a or TDRL-551, Figure 5)

A round-bottom flask coupled with a reflux condenser and containing a dry mixture of 2-chloro-7-ethoxy-3-(3-(4-iodophenyl)-4,5-dihydro-1H-pyrazol-5-yl)quinoline (7a) (0.6 g, 1.25 mmol) and glutaric anhydride (0.14 g, 1.25 mmol) was immersed into a preheated oil bath (65 ^{o}C). $CHCl_3$ (24 mL) was then added through the condenser in one portion. The resulting solution was refluxed for 1.5 h with stirring, after which it was allowed to cool to room temperature. The obtained solid was filtered and washed with ethyl acetate. Further purification by trituration with ethyl acetate yielded acid 9a as an off-white solid (0.53 g, 72%). ^{1}H NMR (500 MHz, DMSO-d_6) d 1.40 (*t*, J=7.0 Hz, 3H), 1.83 (*p*, J=7.5 Hz, 2H), 2.30 (*t*, J=7.5 Hz, 2H), 2.82

(*dt*, J=15.0, 7.5 Hz, 1H), 2.91 (*dt*, J=15.0, 7.5 Hz, 1H), 3.28 (*dd*, J=18.0, 5.5 Hz, 1H), 3.97 (*dd*, J=18.0, 12.0 Hz, 1H), 4.19 (*q*, J=7.0 Hz, 2H), 5.83 (*dd*, J=12.0, 5.5 Hz, 1H), 7.26 (*dd*, J=9.0, 2.5 Hz, 1H), 7.35 (*d*, J=2.5 Hz, 1H), 7.57 (*d*, J=8.5 Hz, 2H), 7.84 (*d*, J=8.5 Hz, 2H), 7.93 (*d*, J=9.0 Hz, 1H), 7.99 (*s*, 1H), 12.09 (*s*, 1H).

2.3. Cell Culture

A2780 cells and A2780/R cells were purchased from Sigma. All other cell lines were from ATCC and routinely tested for mycoplasma contamination. Cells were maintained in RPMI media supplemented with 10% FBS, penicillin and streptomycin. Cultures were incubated at 37 °C in 5% CO_2 and sub-cultured 2-3 times per week.

2.3.1. Clonogenic survival assays

Cells were plated in a 6 well (100,000 cells/well) or 24 well (25,000 cells/well) plate, incubated for at least 18 hours and then treated with Pt/etoposide and/or RPA inhibitors. After 48 hours of treatment, the cells were re-plated in 10 cm dishes (500-1000 cells/dish) and incubated for 8-10 days to allow colony formation. Plates were then washed with PBS, fixed with glutaraldehyde and stained with crystal violet. The colonies were then counted using an Acolyte Synbiosis colony counter.

2.3.2. Assessment of synergy via combination index

In the combination index studies, the A2780 cells were treated with RPA inhibitor and Pt/etoposide alone as well as the combination of both – the inhibitor and the DNA damaging chemotherapeutic agent. The range of treatment was dependent on the IC_{50} of each inhibitor/drug. If the IC_{50} was X, then the cells were

treated at a range of X/4 to 3X concentration in a colony formation assay. The kill curves from both the single agent treatments as well as the combination treatment were used in a Chou-Talalay based method to determine the combination index at different fractions of cells affected (59,60). A CI > 1 indicates antagonism between the two agents, while a CI < 1 indicates synergy. A CI of 1 demonstrates an additive effect.

2.4. Compound-DNA binding assay

A competitive DNA intercalation assay was performed using SYBR-Green. Reactions were carried out in 25 mM MOPS (pH 6.5) containing 30 μM sonicated salmon sperm DNA, SYBR-Green and varying concentrations of RPA inhibitors. Reactions were performed in a black 96-well plate in a final volume of 110 μl. Doxorubicin, a known non-covalent DNA binding chemotherapeutic, was used as a positive control. Fluorescence was measured using a BioTek® Synergy™ H1 hybrid multi-mode microplate reader with an excitation wavelength of 485 nm, emission wavelength of 528 nm and a read height of 7 mm. Data were collected using BioTek® Gen5™ reader software. Reactions were incubated a maximum of 5 minutes before measurements were collected.

2.5. *In vivo* Analysis of TDRL-551

Non-obese diabetic/severe combined immunodeficient mice (NOD/SCID) were obtained from The Jackson Laboratory (http://www.jax.org). All animal studies were conducted under the guidelines of the NIH and were approved by the Institutional Animal Care and Use Committee of Indiana University School of Medicine. Animals were maintained under pathogen-free conditions and a 12-hour

light-dark cycle. The safety and tolerability of TDRL-551 was assessed in naïve NOD/SCID mice. Mice were treated IP with increasing concentrations of TDRL-551 in a formulation consisting of 20% DMSO, 10% Tween 80, 70% PBS. Based on preliminary metabolic profile and a half-life of ~7 hours (data not shown) we administered 3 doses per week for two weeks and measured body weight every other day.

To assess anti-cancer efficacy the hind flanks of sixty 8-10 week old mice were implanted with 2 x 10^6 H460 NSCLC cells in matrigel. Tumor volumes were monitored by caliper measurement [tumor volumes = length x (perpendicular width)^2 x 0.5]. Mice with tumors ranging between 32-152.5mm^3 8 days following implantation were randomized into 4 treatment arms. Carboplatin was dissolved in water and administered via intraperitoneal injection at 50 mg/kg on days 8, 14, and 20 following implantation. TDRL-551 was suspended in 20% DMSO, 10% Tween 80, 70% PBS and administered via intraperitoneal injection at 200 mg/kg biweekly on days 8, 10, 14, 17, and 20. Vehicle controls were administered to arms not receiving indicated treatments. Tumor volumes were monitored biweekly as indicated and the results are presented as the average tumor volume ± standard error of the mean for each group (n=14 per group).

2.6. Statistics

2.6.1. Tolerability of TDRL-551 in NOD/SCID mice.

Student's t test from Sigmaplot was used to test for any statistically significant difference in the overall change in body weight for NOD/SCID mice between each of the TDRL-551 doses and the vehicle treated control. Three mice

were tested for each dosage group (n=3). Each of the data points (days 1, 3, 5, 9, 11, 15, 18) for each of the dosage arms were compared to the corresponding data points in the vehicle treated control. An alpha of 0.05 was used to determine statistical significance.

2.6.2. In vivo anti-cancer activity of TDRL-551.

Unpaired one-tailed student's t test from Sigmaplot was used to determine statistically significant difference in the tumor volumes between each of the treatment arms at the following data points – day 8, 10, 14, 17, 20 and 21. Fourteen mice were used for each of the treatments (n=14). An alpha of 0.05 was used to determine statistical significance.

3. RESULTS

3.1. Screening TDRL-505 analogs

Toward improving the potency and physiochemical properties of TDRL-505, we screened 26 compounds selected on the basis of structural similarity to assess their ability to inhibit RPA-DNA binding activity. These 26 compounds shared the same 2-pyrazoline core structure as TDRL-505, but differed in either the type/length of the side chain attached to N1, the substitution of the phenyl group at C3, or the type of aromatic ring at C5. Data from the 26 compounds are shown in Figures 7A and 8A along with quantification of the data in Figures 7B and 8B. Each of the analogs that displayed inhibitory activity towards RPA was titrated over a range of concentrations to determine IC_{50} values (Figures 7C and 8C). These data were used to determine SAR. We identified three important aspects of the molecules: the length of the carboxylic acid chain, the halogen on the phenyl ring, and the alkyl ether in the quinoline ring (Figure 9). Consequently, we pursued an organic synthesis scheme to prepare additional TDRL-505 analogs and further interrogate the structure activity relationships.

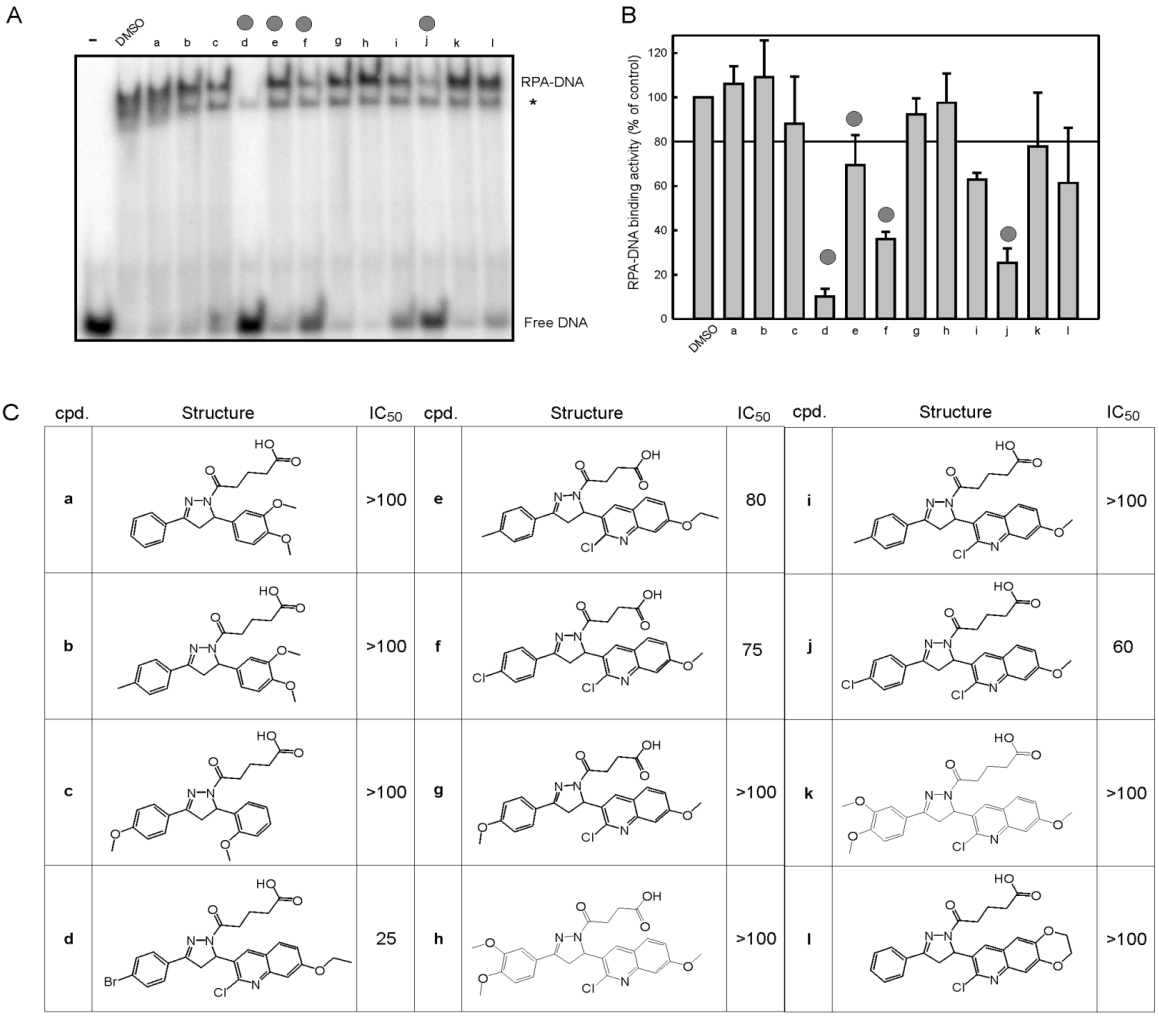

Figure 7: EMSA screening of TDRL-505 analogs-I. (A) 12 TDRL-505 analogs were screened using the EMSA assay for RPA-DNA inhibition activity at 100 μM. The free DNA and RPA-DNA complexes are indicated. The * indicated the position of the E. coli SSB-DNA complex. Quantification of duplicate determinations were averaged and plotted as a percent of control with bars representing the range of values. (C) Structures of compounds with their corresponding IC50 values (μM) calculated from EMSA reactions as described in Methods. Compounds were titrated at a range of 1-125 μM. Compounds indicated with circles in 'A' and 'B' gave us our key preliminary findings in SAR studies. The horizontal line in 'B' represents an 80% cut-off.

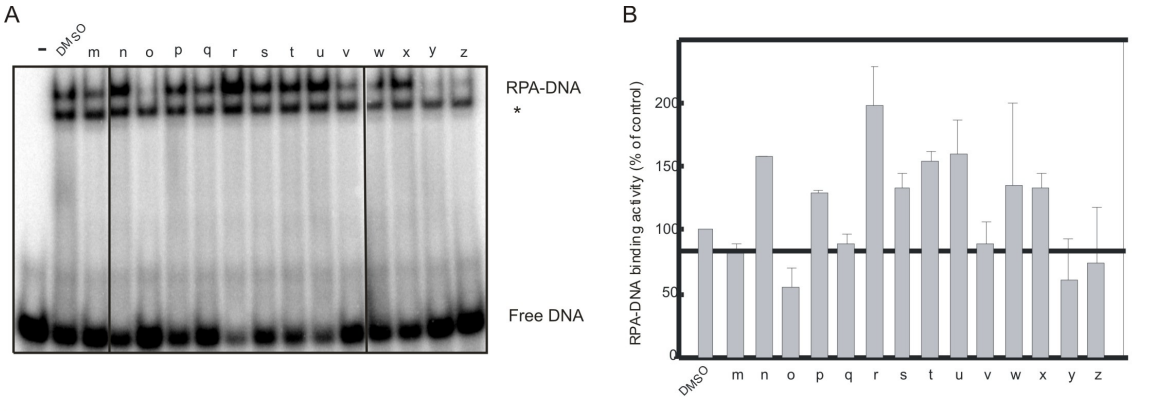

C

cpd.	Structure	IC50	cpd.	Structure	IC50	cpd.	Structure	IC50
m	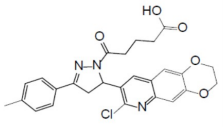	>100	r	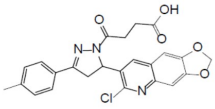	>100	w	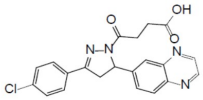	>100
n	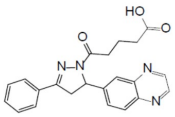	>100	s	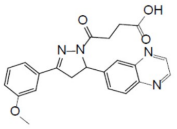	>100	x	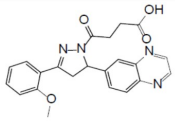	>100
o	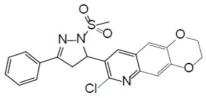	87.5	t	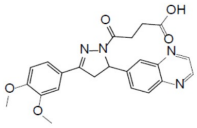	>100	y	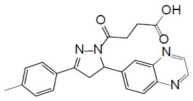	>100
p	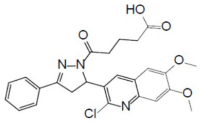	>100	u	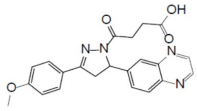	>100	z	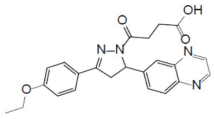	>100
q	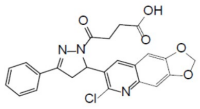	>100	v	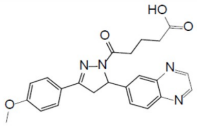	>100	505	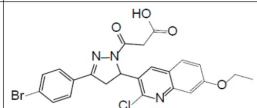	38

Figure 8: EMSA screening of TDRL-505 analogs-II. (A) 14 TDRL-505 analogs were screened using the EMSA assay for RPA-DNA inhibition activity at 100 μM as in Figure 2 A. Quantification of duplicate determinations were averaged and plotted as a percent of control with bars representing the range of values. (C) Structures of compounds with their corresponding IC50 values (μM) calculated from EMSA reactions as described in Methods. Compounds were titrated at a range of 1-125 μM. The horizontal line in 'B' represents an 80% cut-off.

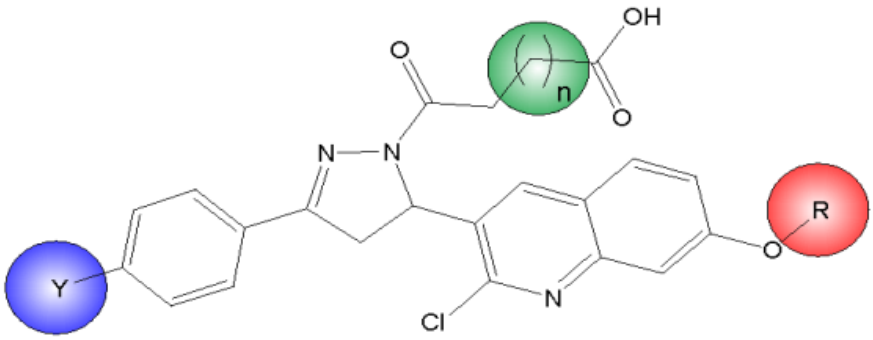

Figure 9: Structural components of TDRL-505 important for potent inhibition of RPA-DNA interaction. The three circles highlight three different aspects of the structure of the small molecule inhibitor that were found to be important in the EMSA based SAR studies.

3.2. Chemistry

The synthetic approach developed for the preparation of TDRL-505 analogs is depicted in Figure 10 and involved 5 steps. Quinolines carbaldehydes **4** were prepared by acylation of alkoxyanilines **2** with acetic anhydride **1**, followed by Vilsmeier-Haack formylation (61). Aldol condensation/dehydration with a corresponding methyl ketone **5** and sodium hydroxide yielded enones **6**, which, upon treatment with hydrazine, afforded 2-pyrazolines **7**. Lastly, acylation at N1 of the pyrazoline core with a cyclic anhydride **8** furnished oxoacids **9**. The list of all the synthesized TDRL-505 analogs is shown in Table1.

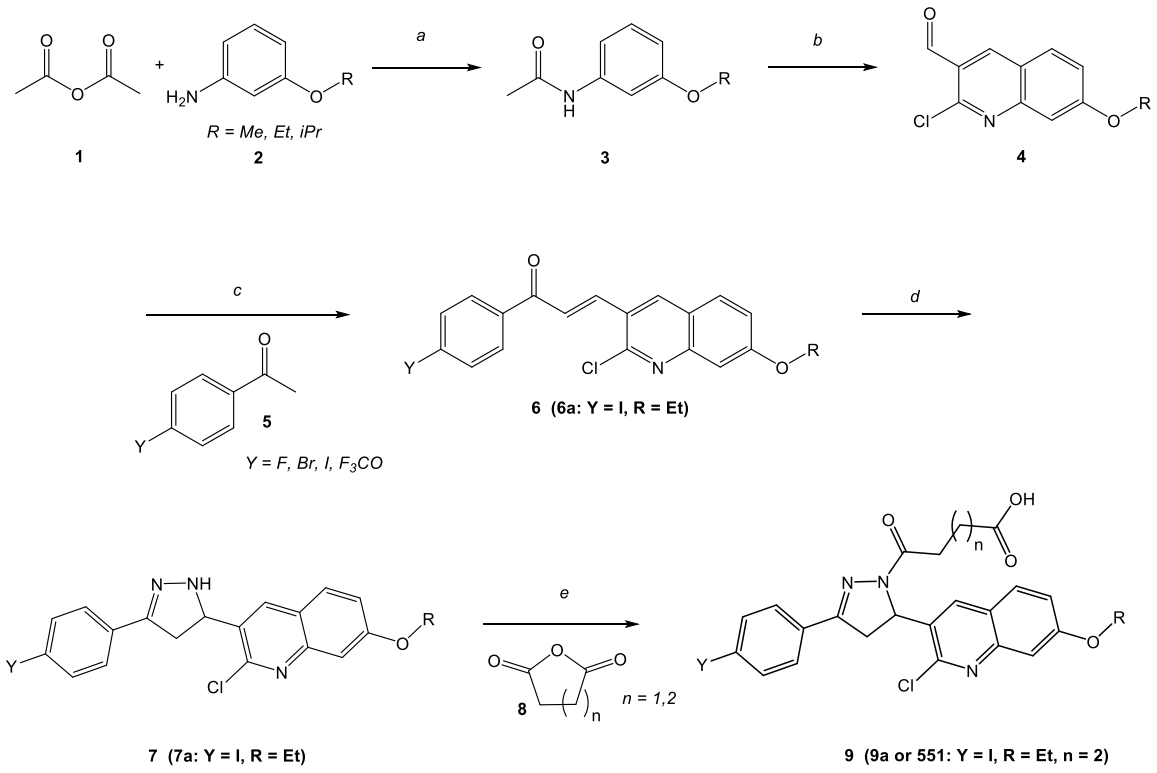

Figure 10: Synthesis of TDRL-505 analogs. Reagents and conditions: (a) DIEA, DMAP, DCM, rt, 2 h, 90-100%. (i) DMF, $POCl_3$, 0 ^oC, 20 min, (ii) Amide, 110 ^oC, 2.5 h, 44-64%. (c) NaOH 10%, EtOH, 45 ^oC, 45 min. (d) $H_2N\text{-}NH_2.H_2O$, EtOH, reflux, 1.5 h, 73-81% (over 2 steps). (e) $CHCl_3$, reflux 1.5 h, 40-72%.

ENTRY	COMPOUND	Y	R	n	*In vitro* IC_{50} (μM)	Cellular IC_{50} (μM)
1	**TDRL-505**	***p*-Br**	**Et**	**1**	**38**	**>50**
2	TDRL-533	*p*-Br	Me	1	>50	>50
3	TDRL-540	*p*-F	Me	1	>100	---
4	TDRL-543	*p*-Br	Et	2	25	50
5	TDRL-539	*p*-F	Me	2	>100	---
6	TDRL-534	*p*-Br	Me	2	35	---
7	TDRL-556	*p*-Br	*i*Pr	2	43	---
8	**TDRL-551**	***p*-I**	**Et**	**2**	**18**	**25**
9	TDRL-557	*p*-F_3CO	Et	2	30	---
10	TDRL-652	*m*-I	Et	2	15	---
11	TDRL-617	*See below*			>100	---
12	TDRL-634	*See below*			>100	---

TDRL-617

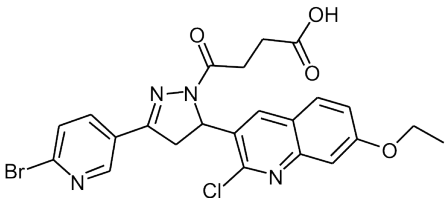

TDRL-634

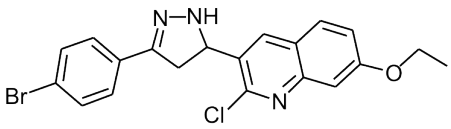

Table 1: *In vitro* and cellular IC_{50} values of TDRL-505 and its analogs. The *in vitro* IC_{50} values are based on EMSA reactions as described in Methods. RPA was incubated with the above compounds at concentration range of 1-125 μM. The cellular IC_{50} values are calculated from clonogenic survival assays as described in Methods. The cells were treated with the above compounds at a concentration range of 1-200 μM. Only four compounds were tested for cellular activity, the rest are indicated with 'na' meaning data not available since the experiments were not performed.

3.3. *In vitro* inhibition of RPA's DNA binding activity

The *in vitro* inhibition of RPA's DNA binding activity was determined by titrating all synthesized TDRL-505 analogs over a range of concentrations from 0-125 μM in an EMSA based assay (Table 1). We observed a slight increased potency by addition of a methylene group to the oxocarboxylic acid moiety *(entries 1 and 4, and 2 and 6)*. Additionally, we found a strong correlation between the identity of the halogen atom on the phenyl ring and the effectiveness of the compound. Iodine imparted the best inhibitory activity, followed by bromine, chlorine *(data not shown)* and fluorine, in that order (*entries 2 and 3, 4 and 8, and 5 and 6)*. The pattern of halo-substitution on the phenyl ring was also evaluated. Since the *meta*-iodo isomer did not exhibit any effect over its *para* analog *(entries 8 and 10)*, we pursued the latter due to its simpler purification process. Lastly, a fluorinated substituent, the trifluoromethoxy group, did not alter the potency of the compound when compared to the parental bromo substitution *(entries 4 and 9)*. Another part of the molecule that was subject of analysis was the alkyl ether moiety on the quinoline ring. The replacement of the ethyl group by either a methyl or isopropyl counterpart resulted in a slight decrease in inhibitory activity *(entries 1 and 2, and 4, 6 and 7)*. Of all analogs tested, TDRL-551 *(entry 8)* exhibited the highest *in vitro* potency, as well as cellular efficacy.

To interrogate the most potent compound TDRL-551 we directly compared its activity of its predecessor TDRL-505. The data presented in Figure 11A compare the EMSA based *in vitro* inhibitory activity of TDRL-551 with that of TDRL-505. The IC_{50} values, calculated form the plotted graphs (Figure 11B), were found to be 18

and 38 μM, respectively, making TDRL-551 greater than twice as potent than its predecessor.

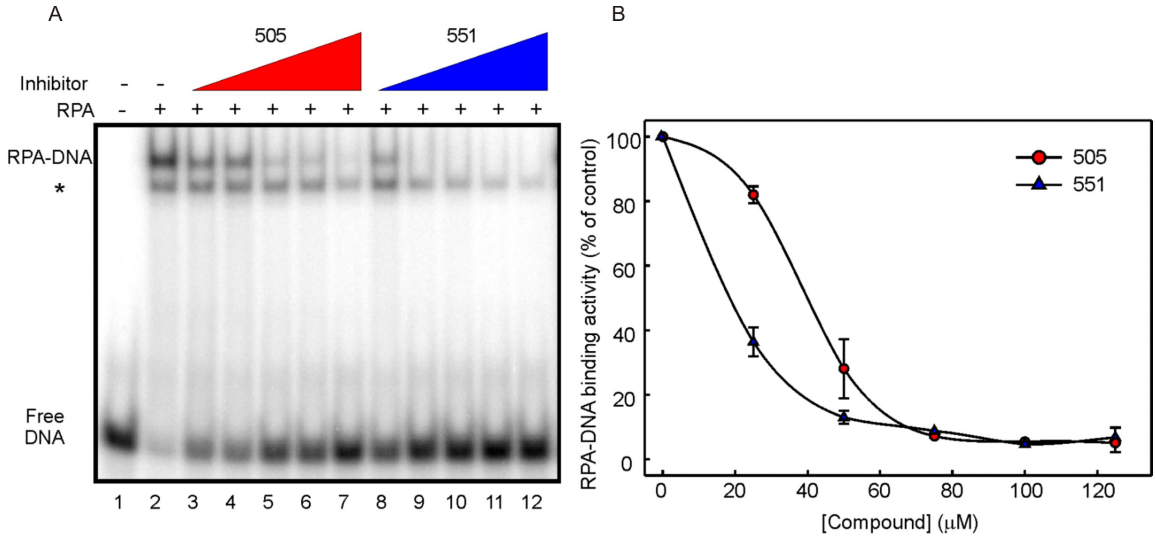

Figure 11: *In vitro* analysis of TDRL-551 inhibitory activity for RPA. A) RPA was incubated with compounds TDRL-505 and TDRL-551 ranging from 1-125 μM. DNA binding was analyzed by EMSA as described in Methods. The position of free DNA and the DNA–RPA complex is denoted in the figure. The * indicated the position of the E. coli SSB-DNA complex. B) Quantification of the data presented in panel A. Data represent the average and SD of three independent determinations and the data were fitted using non-linear regression analysis (Sigmaplot) to obtain IC_{50} values.

The two potential mechanisms for inhibition are either a direct interaction with the protein or an interaction with the DNA that renders it unable to bind to the protein. While our previous results suggested that the 505 class of compounds inhibits DNA binding activity via a direct interaction with the protein RPA, we

sought to determine if TDRL-551 employed the same mechanism. We therefore assessed the ability of TDRL-551 to bind to DNA directly using a fluorescence displacement assay. The results presented in Figure 12 demonstrate that no DNA binding activity was observed. These data support our hypothesis that the compound inhibits the protein-DNA interaction by binding directly to the RPA protein and not via binding to the DNA.

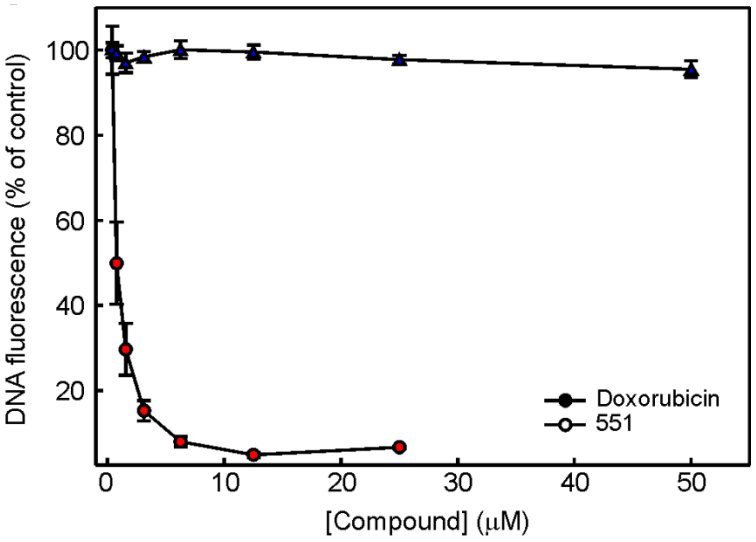

Figure 12: Fluorescent displacement assay. Assays were performed as described and the indicated concentration of 551 or doxorubicin was titrated into reactions containing DNA and SybrGreen. The fluorescence was measured and data represent the average and SD of three independent determinations.

To further delve into the mechanism of binding, we tested whether TDRL-551 could inhibit RPA DBD-A/B binding (the major high affinity DNA binding core) to DNA. Both TDRL-551 and TDRL-505 inhibit RPA DBD-A/B-DNA interaction and hence employ a similar inhibition mechanism (Figure 13). Interestingly, we did not

observe a significant difference in the inhibition potency of TDRL-505 and TDRL-551 for RPA DBD-A/B. We speculate the improved potency of TDRL-551 for full length RPA could be due to its binding at other sites in RPA and thus the overall potency of the molecule could be a result of multiple binding sites.

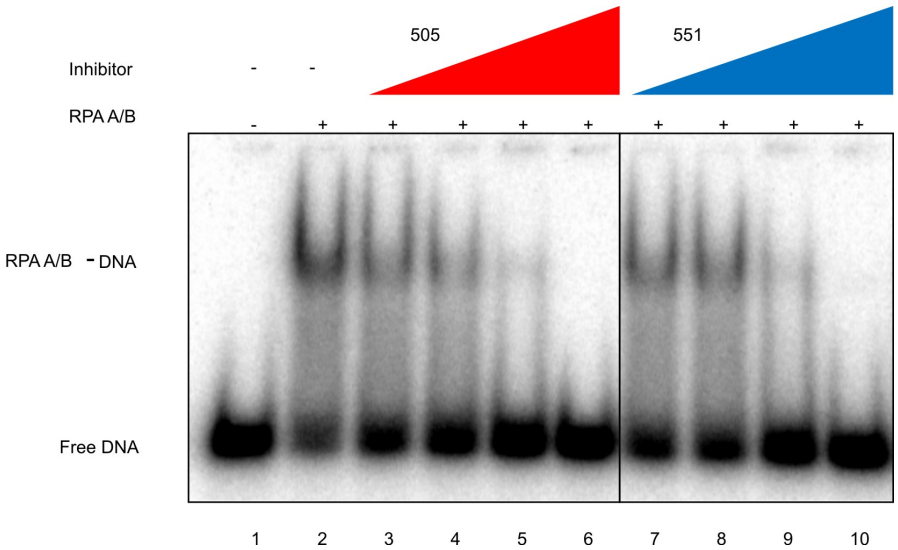

Figure 13: *In vitro* analysis of TDRL-551 inhibitory activity for RPA-A/B Box. RPA-A/B Box was incubated with compounds TDRL-505 and TDRL-551 ranging from 25-100 μM. DNA binding was analyzed by EMSA as described in Methods. The position of free DNA and the DNA–RPA A/B complex is denoted in the figure.

3.4. Cellular activity of TDRL-551

3.4.1. *Single agent anti-cancer activity of RPA inhibitors in EOC cell line*

Considering the essential role of RPA in S-phase DNA replication (62) and our previous data with both reversible and irreversible RPA inhibitors (55,56,58), we evaluated the TDRL-505 analogs for single agent anti-cancer activity in the A2780 EOC cell line using clonogenic survival assays (Table 1). Consistent with our *in vitro* EMSA based studies, TDRL-551 showed the best single agent activity in

these cells. Also in line with the *in vitro* results was the relative cellular inhibitory activity of all tested compounds. Figure 14 shows the data obtained from clonogenic survival assays, comparing the single agent activity of our original lead TDRL-505 and our optimized lead, TDRL-551. TDRL-505's IC_{50} was found to be 55 μM, while TDRL-551 was twice as potent with an IC_{50} of 25 μM. Interestingly, the degree of improvement in potency remained consistent between the *in vitro* and cellular assays.

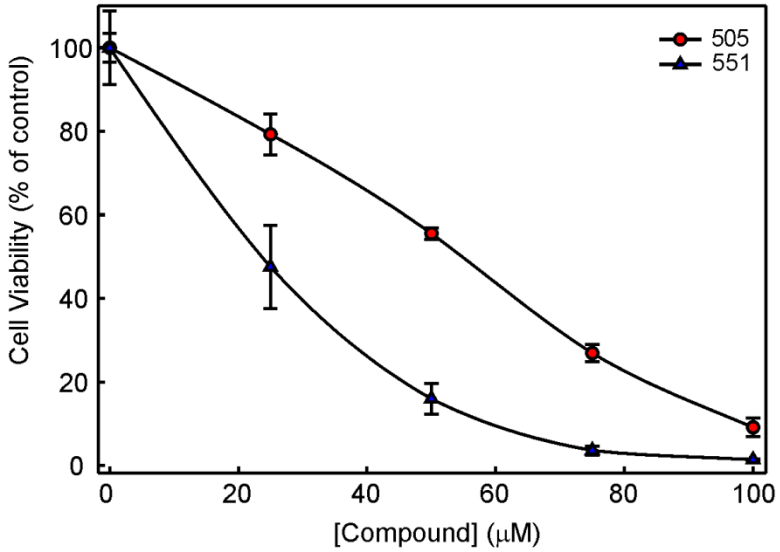

Figure 14: Cellular activity of TDRL-505 and TDRL-551 in A2780. A2780 cells were treated with RPA inhibitor TDRL-505 or TDRL-551 for 48 hours and viability was assessed in a colony formation assay as described in Methods. The colonies were counted and normalized to the untreated controls to determine cellular viability. The data represent the average and SEM from three independent determinations and the data were fit using non-linear regression analysis (Sigmaplot) to calculate cellular IC_{50}s.

To ensure that the activity was not cell line specific, we also assessed the single agent activity of TDRL-551 in three other EOC cell lines, SKOV3 and OVCA429 (ATCC) both of which were isolated from patients with recurrent ovarian cancer following platinum therapy and the cisplatin resistant A2780 derivative (63). We also assessed activity in the H460 NSCLC cell line. In each case, TDRL-551 displayed single agent activity similar to that observed in the parental A2780 EOC cells (Figure 15) demonstrating that, as would be expected for an RPA inhibitor, the mode of activity is not restricted to a single cell line or cancer type.

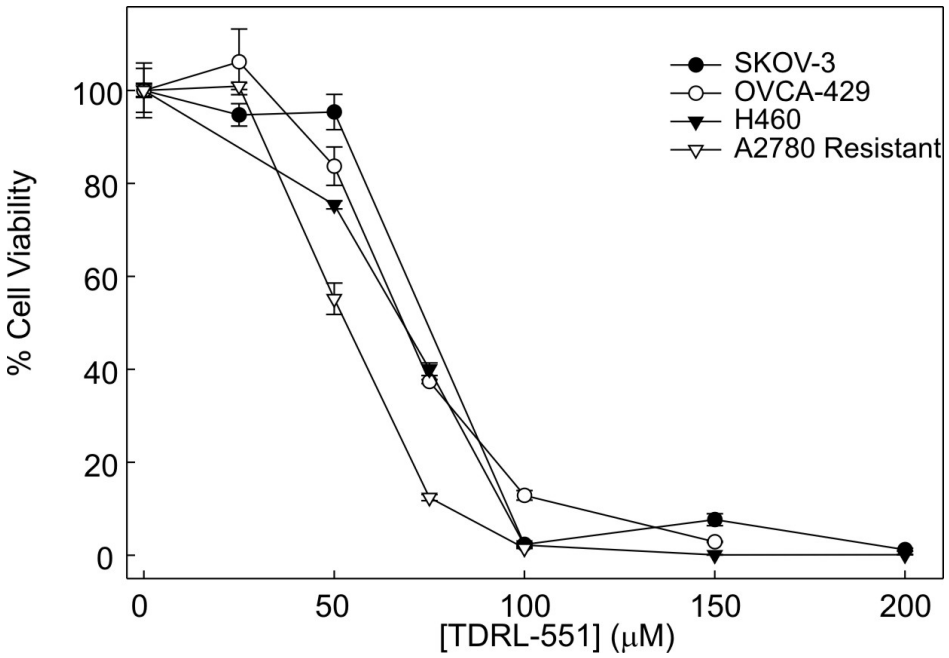

Figure 15: Analysis of TDRL551 single agent activity in H460 NSCLC, SKOV3, A2780/R and OVCA429 EOC cells. A2780 cells were treated with RPA inhibitor TDRL-505 or TDRL-551 for 48 hours and viability was assessed in a colony formation assay as described in Methods. The colonies were counted and normalized to the untreated controls to determine cellular viability. The data

represent the average and SEM from three independent determinations and the data were fit using non-linear regression analysis (Sigmaplot) to calculate cellular IC_{50}s.

3.4.2. *Synergy with DNA damaging chemotherapeutic agents in EOC*

Since repair and tolerance of Pt-DNA lesions predominantly occur via NER and HR, cellular inhibition of RPA should have a dramatic effect on the sensitization of cancer cells to Pt. In order to determine whether inhibition of RPA with TDRL-551 synergizes with Pt in EOC cells, we performed combination treatment studies with TDRL-551 and cisplatin. We used the platinum sensitive A2780 cell line as our cell culture model for EOC. Figure 16 shows the dose-response curves for the combination treatment of TDRL-551 and cisplatin along with the appropriate single agent controls from a representative experiment. An average of three biological replicate experiments for combination studies of TDRL-551 with Pt in A2780 cell line was performed to determine the combination index (Figure 18). Our data show a synergistic effect indicated by a CI < 1 at 0.5 or higher fraction of cells affected. The data obtained are consistent with our hypothesis that RPA inhibition makes cancer cells more sensitive towards Pt and hence acts synergistically with cisplatin treatment.

Since RPA also plays a crucial role in replication, we also tested TDRL-551 in combination with etoposide, a topoisomerase II inhibitor. Figure 17 demonstrates the dose-response curves for the combination treatment of TDRL-551 and etoposide along with the appropriate single agent controls from a representative experiment.

An average of three biological replicate experiments for combination studies of TDRL-551 with etoposide in A2780 cell line was performed to determine the combination index. TDRL-551 was mildly synergistic with etoposide at the highest fraction of cells affected (> 0.8) (Figure 18).

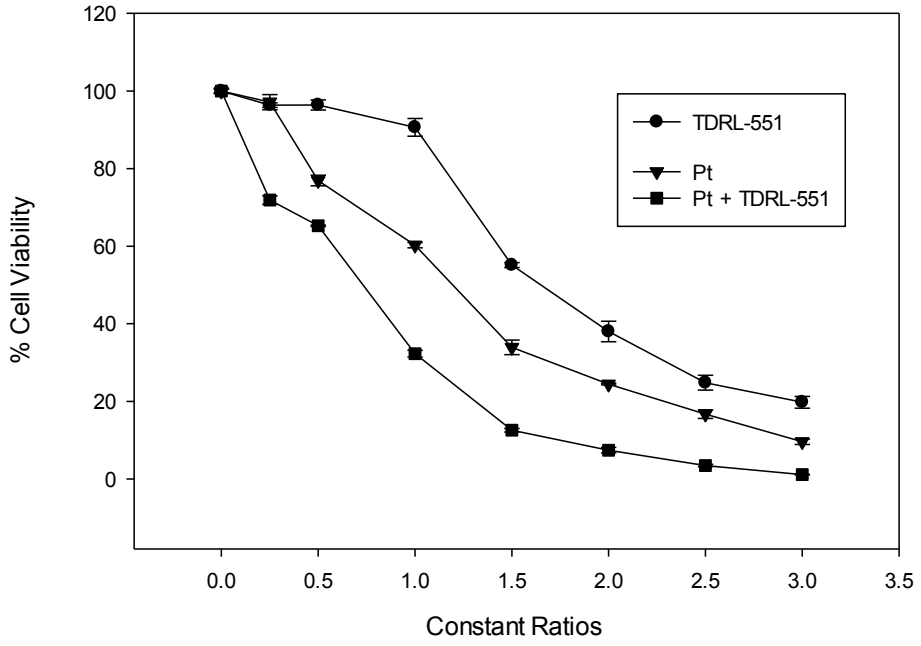

Figure 16: Dose-response curves for TDRL-551 and Pt. Cell viability was determined from clonogenic survival assays for TDRL-551 and Pt combination treatment along with single agent controls in A2780 cell line as described in the Methods. Constant Ratio of 1 equals 40 μM for TDRL-551 and 1.5 μM for Pt. The data is from a representative experiment from a set of three independent biological replicates.

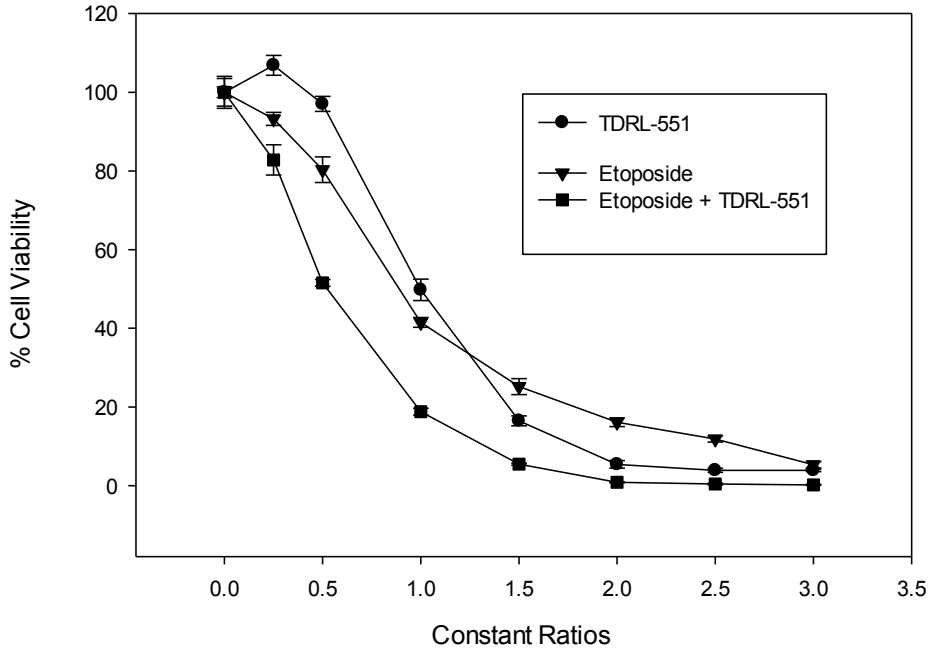

Figure 17: Dose-response curves for TDRL-551 and etoposide. Cell viability was determined from clonogenic survival assays for TDRL-551 and etoposide combination treatment along with single agent controls in A2780 cell line as described in the Methods. Constant Ratio of 1 equals 60 μM for TDRL-551 and 75 nM for etoposide. The data is from a representative experiment from a set of three independent biological replicates.

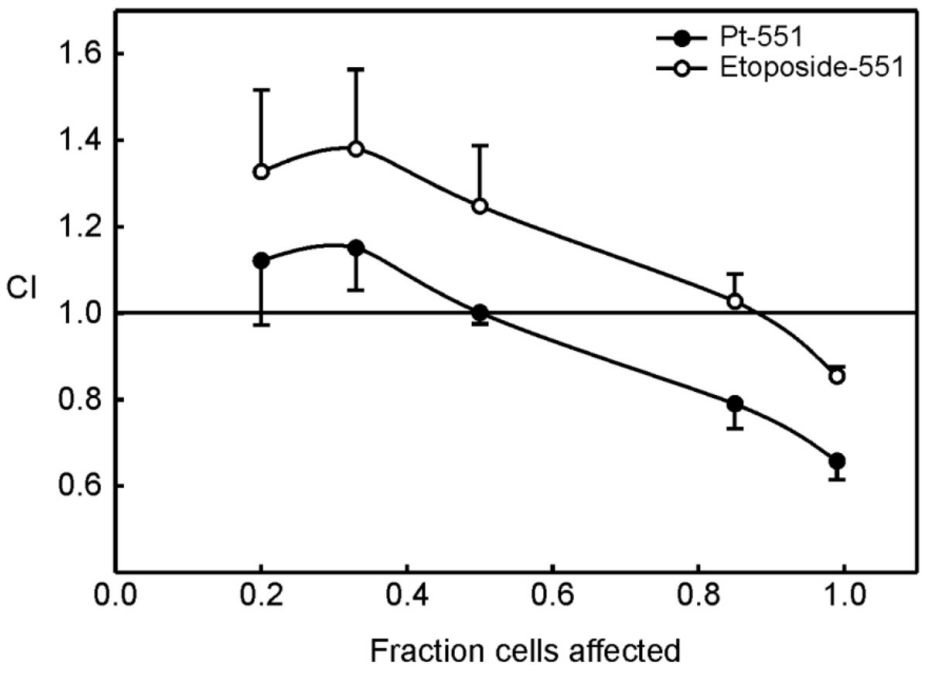

Figure 18: The CI of TDRL-551 with Pt and etoposide. CIs were determined through a Chou-Talalay based approach as described in the Methods. The data represent the average and SEM from three independent determinations.

3.5. RPA Inhibitor TDRL-551 displays single agent anti-cancer activity and sensitizes NSCLC tumors to platinum based treatment *in vivo*.

To determine the effect of RPA inhibition via TDRL-551 treatment *in vivo* we first assessed tolerability and experiments demonstrated no body-weight loss with intraperitoneal administration up to 200 mg/kg (Figure 19). A slight decrease in body weight was observed at 300 mg/kg, but was not statistically significant. Co-treatment with carboplatin was also assessed and again, no adverse effects or loss of weight was observed up to 200 mg/kg (data not shown). We then determined anti-cancer activity in H460 NSCLC xenografts. Initial pharmacokinetic analysis revealed

that ability to achieve a plasma concentration of >20 μM with a half-life of over 7 hours (data not shown).

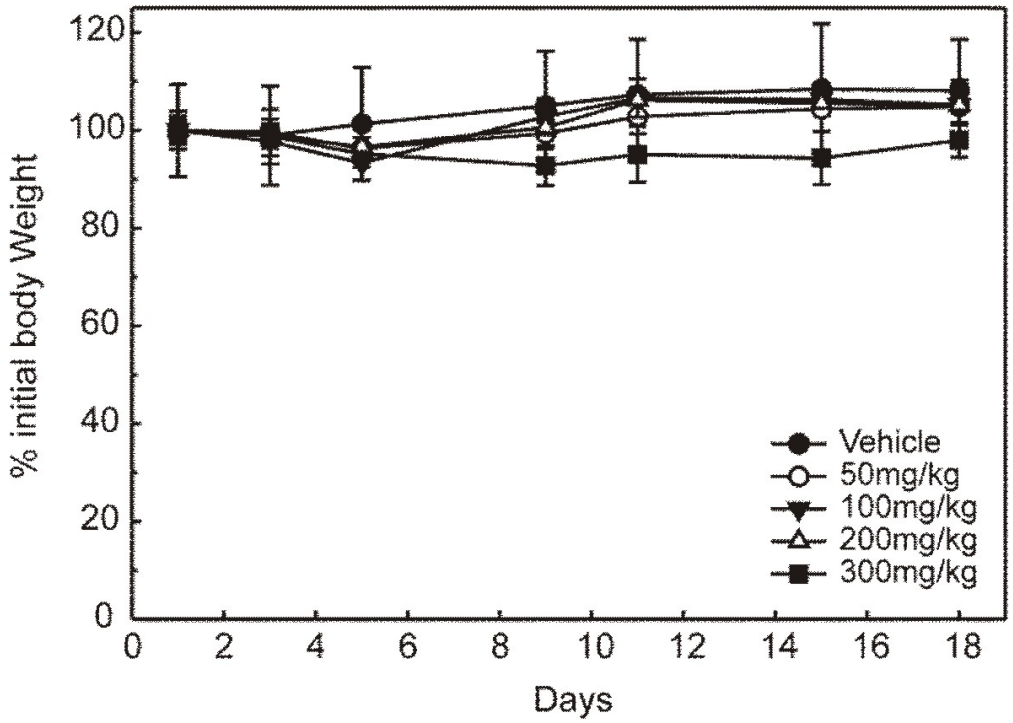

Figure 19: Overall change in body-weight in response to treatment with TDRL-551. Tolerability of TDRL-551 was assessed via body weight determinations following triweekly dosing at the indicated drug concentrations. Mice were treated on days 1, 3, 5, 8, 10, and 12 IP as described in Methods. Data are reported as the percent of body weight on day 1 and represent the mean ± standard error of the mean (n=3). There was no statistically significant difference between each of the treatment arms compared to vehicle control as determined by student's t test described in methods.

Tumor cells were therefore implanted in NOD/SCID mice that were randomized and treated with vehicle, TDRL-551; carboplatin; or the combination of

TDRL-551 and carboplatin (Figure 20). Carboplatin is often used in the treatment of NSCLC and forms DNA adducts chemically indistinguishable from those forms with cisplatin. As a result of the similarity in the DNA adducts formed between carboplatin and cisplatin, the repair pathways that impact sensitivity are identical. Tumor volumes were monitored for 2 weeks following initiation of treatment regimens and averages for each treatment arm are reported. Each of the treatment arms is clearly distinct from the untreated control group. The tumor volumes for all treatment arms at all data points post day 8 were statistically different from the tumor volumes for the corresponding data points in the vehicle control, apart from carboplatin treatment on day 14. Carboplatin treatment and TDRL-551 displayed similar growth inhibition of tumors. There was no statistically significant difference at any of the data points between carboplatin and TDRL-551 treatment. This demonstrates single agent anti-cancer activity of TDRL-551 *in vivo* that is consistent with the cellular assays reported above. Interestingly, mice receiving carboplatin and TDRL-551 demonstrated the slowest tumor growth, consistent with TDRL-551 sensitizing cells to platinum. The difference in the tumor volumes between the combination treatment and TDRL-551 alone was statistically significant at all data points post day 14. However, the tumor volumes for carboplatin and the combination treatment were statistically different only at day 17. The variation in the initial tumor volumes (range = 120.5 mm^3) may partially explain the huge variation in the tumor volumes at day 20 and 21 and hence the statistics. These data demonstrate single agent activity for TDRL-551 *in vivo* in NSCLC tumors and a potential to sensitize these tumors to Pt-based therapy.

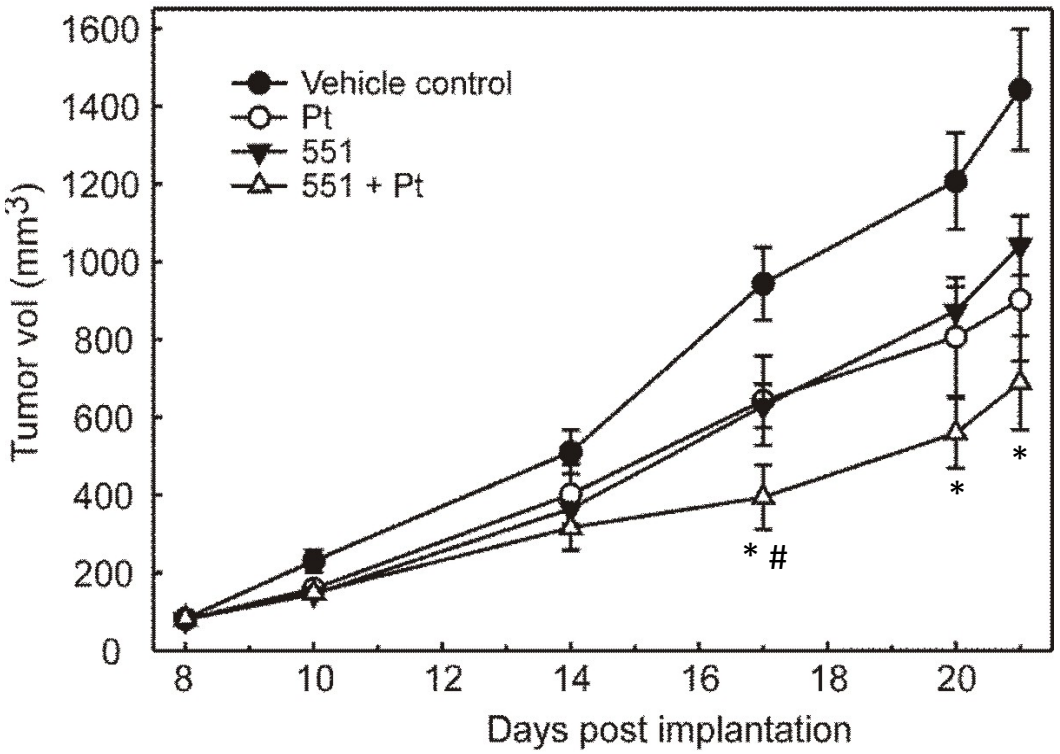

Figure 20: *In vivo* anti-cancer activity of TDRL-551. *In vivo* anti-cancer activity was assessed in human H460 NSCLC tumor xenografts in NOD/SCID mice. Mice were implanted on day 1, tumor measured by calipers and individual mice randomly assigned to one of 4 treatment arms. Carboplatin was administered once per week on days 8, 14 and 20. TDRL 551 was administered biweekly on days 8, 10, 14, 17, and 20. Tumor volumes were monitored by caliper measurement [tumor volume = length (perpendicular width)^2 x 0.5] biweekly as indicated. Average tumor volume ± standard error of the mean for each group is reported in mm^3 (n=14). The '*' and the '#' indicate statistically significant differences for the combination treatment from the TDRL-551 and carboplatin treatment arms respectively.

4. DISCUSSION

The research presented in this thesis describes the synthesis, structure activity relationships and *in vitro* and cellular activity of novel reversible RPA inhibitors in EOC and NSCLC (Figures 7-15; Table 1). We have demonstrated both single agent activity and synergy in combination with DNA damaging chemotherapeutic agents; cisplatin and etoposide (Figures 16-18). *In vivo* data demonstrate good tolerability and potential therapeutic efficacy in combination with carboplatin in a NSCLC xenograft model (Figures 19-20). This represents the first *in vivo* deployment of a small molecule inhibitor targeting the RPA-DNA interaction. The SARs defined the necessary substituents for activity while maintaining excellent bioavailability (data not shown). These data demonstrate that to achieve *in vivo* activity a balance between potency and bioavailability can lean towards lower affinity as long as PK parameters allow clinically effective concentrations to be maintained. This balance is especially important in targeting RPA an essential protein with homozygous mutations being embryonically lethal in mice, while heterozygous mutants having an early predisposition to cancer (64). No loss of function mutation for RPA has been reported in humans and genetic knockdown of RPA affects cellular viability (62). Consequently, targeting RPA could have potential negative effects on rapidly dividing healthy cells, such as gut epithelial, hematopoietic, or hair follicle, and it could lead to unwanted side effects. For this reason, exploiting the separation of function phenomena in RPA in a manner amenable for therapeutic intervention is crucial. Our laboratory has previously published minimal cytotoxic effects on peripheral blood lymphocytes

with the TDRL-505 inhibitor (58). Moreover, our mouse toxicity studies with TDRL-551 indicate no significant overall change in body weight for doses up to 300 mg/kg, but show anti-tumor activity at the same dosage in a lung cancer xenograft model (Figures 19-20). We hypothesize that since cancer cells are undergoing an abnormal unregulated rate of proliferation, they are in a state of replicative stress and their dependence on RPA can be used to obtain a therapeutic window without harming the normal cells. This can also be understood by analogy to an oncogene addiction model, in which cancer cells have a higher dependence on the oncogene compared to normal cells and hence can be selectively targeted. Finally, RPA's overexpression has been correlated with multiple cancers like breast, lung and colon, and it has also been associated with metastasis (65-68). Thus, clinical reports of altered RPA expression in a variety of cancers make RPA a promising novel therapeutic target.

It is also important to elucidate whether our inhibitors exclusively impair the repair function of RPA without compromising its role in replication. Our previously published data with inhibitor TDRL-505 demonstrate a G1 cell cycle arrest, however the cells those are already in S-phase progress through the replication phase (58). This indicates that our inhibitors are either blocking the initial phase of replication initiation or early origin firing and inhibiting the transition from G1 to S phase, or causing an alteration in the DNA damage checkpoint signaling. In either case, the 505 class of inhibitors do not block progression through S-phase once the G1-S transition has occurred. Our current results demonstrating synergy of TDRL-551 with Pt in an EOC cell line (Figure 18), along with our published data showing

synergy of TDRL-505 with Pt in a lung cancer cell line (58) indicates that our RPA inhibitors are impairing the repair function of RPA. The major limitation for successful treatment of a variety of cancers, including EOC, has been the tolerance and repair of Pt-DNA adducts and has been specifically correlated to increased repair in a variety of ovarian cancer cell lines (69). Hence, inhibiting DNA repair by targeting RPA could have a major significance for cancer therapy.

We also examined the ability of TDRL-551 to synergize with etoposide, a topoisomerase II inhibitor (Figures 17-18). Etoposide treatment leads to both single and double stranded DNA breaks as well as stalling and collapse of replication forks (70,71). Inhibiting RPA's replication function could further enhance the number of DNA breaks produced on etoposide treatment and improve the effectiveness of the treatment. Although TDRL-505 has been previously shown to be highly synergistic with etoposide in lung cancer cells through a flow cytometry based Annexin-PI staining assay (58), its optimized analog, TDRL-551, showed modest synergy with etoposide at the highest fractions of cells affected (> 0.8) in A2780 EOC cell line through colony formation assay (Figure 18). Compound TDRL-551 may be more specific in targeting the repair function of RPA than its predecessor TDRL-505 and hence doesn't significantly impact replication and only mildly synergizes with etoposide. Alternatively, the differences may be a function of the cell lines used and cancer types being investigated. While cisplatin and etoposide are the standard drugs used in treatment against lung cancer, the therapy for ovarian cancer involves the combination of platinum and taxol. Etoposide is not a first line therapy for EOC and hence improving its effectiveness may be limited

based on the cancer. Lastly, we cannot rule out that the differing synergy outcomes are a consequence of the type of assay performed in each case. Despite these caveats, the important finding is that RPA inhibition with TDRL-551 synergizes with cisplatin in EOC and may provide an avenue to increase sensitivity to platinum in the clinic.

RPA inhibitors can be used as DNA repair inhibitors to overcome resistance to platinum based chemotherapies. Inhibiting DNA repair with SMIs can be used in combination with Pt both at first line and second line stage of therapy (Figure 21). In first line therapy, Pt in combination with RPA inhibitors could lead to maximum effectiveness by killing the majority of cancer cells, which are now sensitized to Pt due to inhibition of DNA repair. This may certainly still lead to some surviving cancer cells that are resistant to the treatment due to other mechanisms, such as reduced uptake of platinum, increased drug efflux, or increased expression of proteins like glutathione that bind and inactivate Pt in the cells. However, since there will be less number of surviving cancer cells to relapse with platinum resistant forms, any increase in the effectiveness of the first line therapy would lead to an improved PFS, which can be clinically significant. As second line therapy, RPA inhibitors can be used in combination with Pt to re-sensitize the platinum resistant cancers, also leading to an increase in PFS.

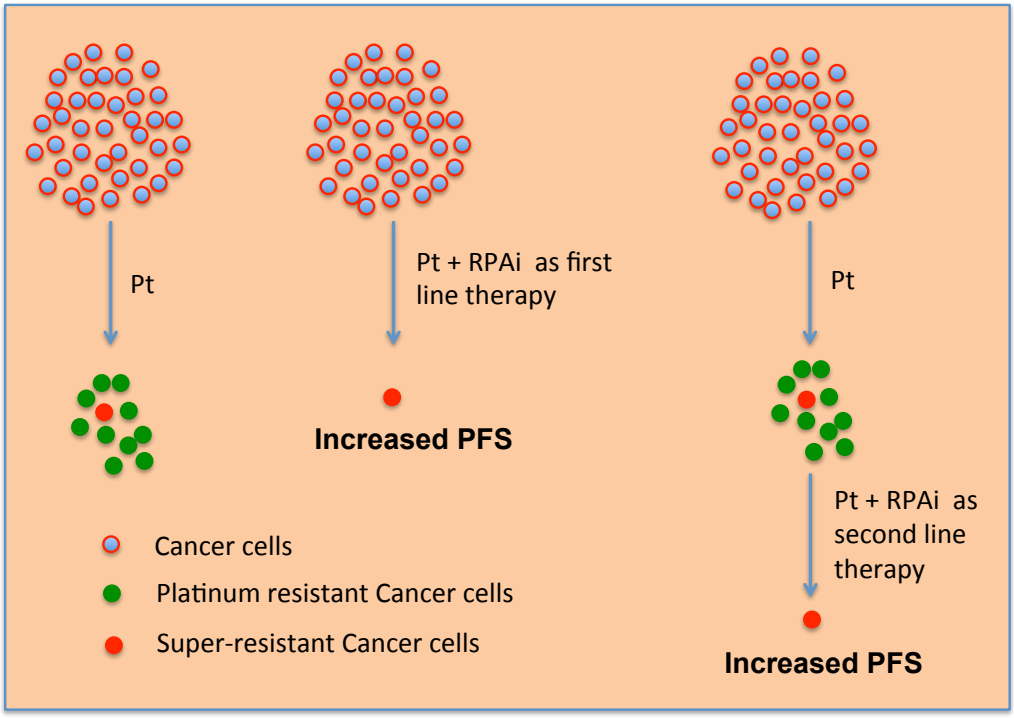

Figure 21: RPA inhibitors (RPAi) as first-line and second-line platinum based combination therapy.

It is important to mention that platinum based chemotherapy is not the only scope for the utility of RPA inhibitors. Since RPA plays a variety of roles in different pathways, its other functions can also be targeted. For instance, RPA inhibitors can be used in combination with radiation therapy that induces DSBs. Thus, inhibiting RPAs role in HR-dependent DSB repair would be expected to enhance the effectiveness of radiotherapy. In conclusion, RPA inhibitors can be used in a multitude of platforms with a special focus in the area of cancer therapy.

Future studies should be directed towards testing the TDRL-551 class of RPA inhibitors for their ability to directly inhibit DNA repair. Inductively coupled plasma

mass spectroscopy technique could be used to determine Pt repair kinetics in cells with and without treatment with RPA inhibitors. This would help in deciphering the mechanism of Pt-sensitization observed in response to these inhibitors. *In vitro* NER assays could be performed to determine whether TDRL-551 class of RPA inhibitors directly inhibit NER. Impact of RPA inhibitors on cellular NER activity can also be determined by the new technique established by Dr. Sancar and group which measures the amount of excised oligonucleotides following NER (72). These assays will provide confirmatory evidence for the inhibition of NER by RPA inhibitors. Similarly, whether inhibition of RPA by small molecule inhibitors inhibits HR can be determined by commercially available HR assay kits. Moreover, Pt-sensitization and the synergistic impact of RPA inhibitors should be measured as a function of HR status. This would help determine the efficacy of these inhibitors in a large subset of ovarian cancers which are HR deficient. A BRCA1 knockdown A2780 cell line would be a great approach to complement our current data to answer the above question. Other BRCA1/2 deficient cell culture models along with their complemented wt counterparts can be used to validate the result in multiple cell lines. Finally, SAR studies can be pursued to obtain more potent and specific inhibitors and further optimize the solubility and bioavailabilty parameters of the current inhibitors. These studies will provide a strong base for the development of small molecule inhibitors targeting RPA-DNA interaction to overcome Pt-resistance at a clinical scale.

References

1. Wiltshaw, E. (1979) Cisplatin in the Treatment of Cancer: The First Metal Anti-Tumor Drug. *Platinum Metals Reveiews* **3**, 90-98
2. Kelland, L. (2007) The resurgence of platinum-based cancer chemotherapy. *Nature reviews. Cancer* **7**, 573-584
3. Hanna, N., and Einhorn, L. H. (2014) Testicular cancer: a reflection on 50 years of discovery. *Journal of clinical oncology : official journal of the American Society of Clinical Oncology* **32**, 3085-3092
4. Galluzzi, L., Senovilla, L., Vitale, I., Michels, J., Martins, I., Kepp, O., Castedo, M., and Kroemer, G. (2012) Molecular mechanisms of cisplatin resistance. *Oncogene* **31**, 1869-1883
5. Ozols, R. F., Bookman, M. A., Connolly, D. C., Daly, M. B., Godwin, A. K., Schilder, R. J., Xu, X., and Hamilton, T. C. (2004) Focus on epithelial ovarian cancer. *Cancer cell* **5**, 19-24
6. Kenfield, S. A., Wei, E. K., Stampfer, M. J., Rosner, B. A., and Colditz, G. A. (2008) Comparison of Aspects of Smoking Among Four Histologic Types of Lung Cancer. *Tobacco Control* **17**, 198-204
7. Ledermann, J. A., and Kristeleit, R. S. (2010) Optimal treatment for relapsing ovarian cancer. *Annals of oncology : official journal of the European Society for Medical Oncology / ESMO* **21 Suppl 7**, vii218-222
8. (2014) Recurrent or Persistent Ovarian Epithelial Cancer Treatment. in *Ovarian Epithelial Cancer Treatment (PDQ®)*, NCI, http://www.cancer.gov/cancertopics/pdq/treatment/ovarianepithelial/HealthProfessional/page6
9. Leamon, C. P., Lovejoy, C. D., and Nguyen, B. (2013) Patient selection and targeted treatment in the management of platinum-resistant ovarian cancer. *Pharmacogenomics and personalized medicine* **6**, 113-125
10. Shanker, M., Willcutts, D., Roth, J. A., and Ramesh, R. (2010) Drug resistance in lung cancer. *Lung Cancer: Targets and Therapy* **1**, 23-36
11. Subramanian, J., and Govindan, R. (2007) Lung cancer in never smokers: a review. *Journal of clinical oncology : official journal of the American Society of Clinical Oncology* **25**, 561-570
12. Popper, H. H. (2011) Large cell carcinoma of the lung – a vanishing entity? *Memo - Magazine of European Medical Oncology* **4**, 4-9
13. Jones, C., and Earnhardt, P. (2007) Targeted Therapies for NSCLC. *US Pharm* **32**, 5-13
14. Bayraktar, S., and Rocha-Lima, C. M. (2013) Molecularly targeted therapies for advanced or metastatic non-small-cell lung carcinoma. *World journal of clinical oncology* **4**, 29-42
15. Koberle, B., Tomicic, M. T., Usanova, S., and Kaina, B. (2010) Cisplatin resistance: preclinical findings and clinical implications. *Biochimica et biophysica acta* **1806**, 172-182

16. Henkels, K. M., and Turchi, J. J. (1997) Induction of apoptosis in cisplatin-sensitive and -resistant human ovarian cancer cell lines. *Cancer research* **57**, 4488-4492
17. Henkels, K. M., and Turchi, J. J. (1999) Cisplatin-induced apoptosis proceeds by caspase-3-dependent and -independent pathways in cisplatin-resistant and -sensitive human ovarian cancer cell lines. *Cancer research* **59**, 3077-3083
18. Siddik, Z. H. (2003) Cisplatin: mode of cytotoxic action and molecular basis of resistance. *Oncogene* **22**, 7265-7279
19. Norbury, C. J., and Zhivotovsky, B. (2004) DNA damage-induced apoptosis. *Oncogene* **23**, 2797-2808
20. Husain, A., He, G., Venkatraman, E. S., and Spriggs, D. R. (1998) BRCA1 up-regulation is associated with repair-mediated resistance to cis-diamminedichloroplatinum(II). *Cancer research* **58**, 1120-1123
21. Ishida, S., McCormick, F., Smith-McCune, K., and Hanahan, D. (2010) Enhancing tumor-specific uptake of the anticancer drug cisplatin with a copper chelator. *Cancer cell* **17**, 574-583
22. Samimi, G., Safaei, R., Katano, K., Holzer, A. K., Rochdi, M., Tomioka, M., Goodman, M., and Howell, S. B. (2004) Increased expression of the copper efflux transporter ATP7A mediates resistance to cisplatin, carboplatin, and oxaliplatin in ovarian cancer cells. *Clinical cancer research : an official journal of the American Association for Cancer Research* **10**, 4661-4669
23. Yamasaki, M., Makino, T., Masuzawa, T., Kurokawa, Y., Miyata, H., Takiguchi, S., Nakajima, K., Fujiwara, Y., Matsuura, N., Mori, M., and Doki, Y. (2011) Role of multidrug resistance protein 2 (MRP2) in chemoresistance and clinical outcome in oesophageal squamous cell carcinoma. *British journal of cancer* **104**, 707-713
24. Ferry, K. V., Hamilton, T. C., and Johnson, S. W. (2000) Increased nucleotide excision repair in cisplatin-resistant ovarian cancer cells: role of ERCC1-XPF. *Biochemical pharmacology* **60**, 1305-1313
25. Reardon, J. T., Vaisman, A., Chaney, S. G., and Sancar, A. (1999) Efficient nucleotide excision repair of cisplatin, oxaliplatin, and Bis-aceto-ammine-dichloro-cyclohexylamine-platinum(IV) (JM216) platinum intrastrand DNA diadducts. *Cancer research* **59**, 3968-3971
26. Koberle, B., Masters, J. R., Hartley, J. A., and Wood, R. D. (1999) Defective repair of cisplatin-induced DNA damage caused by reduced XPA protein in testicular germ cell tumours. *Current biology : CB* **9**, 273-276
27. Vaisman, A., Varchenko, M., Umar, A., Kunkel, T. A., Risinger, J. I., Barrett, J. C., Hamilton, T. C., and Chaney, S. G. (1998) The role of hMLH1, hMSH3, and hMSH6 defects in cisplatin and oxaliplatin resistance: correlation with replicative bypass of platinum-DNA adducts. *Cancer research* **58**, 3579-3585
28. Wang, H., Zhang, S. Y., Wang, S., Lu, J., Wu, W., Weng, L., Chen, D., Zhang, Y., Lu, Z., Yang, J., Chen, Y., Zhang, X., Chen, X., Xi, C., Lu, D., and Zhao, S. (2009) REV3L confers chemoresistance to cisplatin in human gliomas: the potential of its RNAi for synergistic therapy. *Neuro-oncology* **11**, 790-802

29. Deans, A. J., and West, S. C. (2011) DNA interstrand crosslink repair and cancer. *Nature reviews. Cancer* **11**, 467-480
30. Alli, E., Sharma, V. B., Hartman, A. R., Lin, P. S., McPherson, L., and Ford, J. M. (2011) Enhanced sensitivity to cisplatin and gemcitabine in Brca1-deficient murine mammary epithelial cells. *BMC pharmacology* **11**, 7
31. Taniguchi, T., Tischkowitz, M., Ameziane, N., Hodgson, S. V., Mathew, C. G., Joenje, H., Mok, S. C., and D'Andrea, A. D. (2003) Disruption of the Fanconi anemia-BRCA pathway in cisplatin-sensitive ovarian tumors. *Nature medicine* **9**, 568-574
32. Vousden, K. H., and Lane, D. P. (2007) p53 in health and disease. *Nature reviews. Molecular cell biology* **8**, 275-283
33. Erovic, B. M., Pelzmann, M., Grasl, M., Pammer, J., Kornek, G., Brannath, W., Selzer, E., and Thurnher, D. (2005) Mcl-1, vascular endothelial growth factor-R2, and 14-3-3sigma expression might predict primary response against radiotherapy and chemotherapy in patients with locally advanced squamous cell carcinomas of the head and neck. *Clinical cancer research : an official journal of the American Association for Cancer Research* **11**, 8632-8636
34. Han, J. Y., Hong, E. K., Choi, B. G., Park, J. N., Kim, K. W., Kang, J. H., Jin, J. Y., Park, S. Y., Hong, Y. S., and Lee, K. S. (2003) Death receptor 5 and Bcl-2 protein expression as predictors of tumor response to gemcitabine and cisplatin in patients with advanced non-small-cell lung cancer. *Medical oncology* **20**, 355-362
35. Michaud, W. A., Nichols, A. C., Mroz, E. A., Faquin, W. C., Clark, J. R., Begum, S., Westra, W. H., Wada, H., Busse, P. M., Ellisen, L. W., and Rocco, J. W. (2009) Bcl-2 blocks cisplatin-induced apoptosis and predicts poor outcome following chemoradiation treatment in advanced oropharyngeal squamous cell carcinoma. *Clinical cancer research : an official journal of the American Association for Cancer Research* **15**, 1645-1654
36. Williams, J., Lucas, P. C., Griffith, K. A., Choi, M., Fogoros, S., Hu, Y. Y., and Liu, J. R. (2005) Expression of Bcl-xL in ovarian carcinoma is associated with chemoresistance and recurrent disease. *Gynecologic oncology* **96**, 287-295
37. Friedman, E. (2007) Mirk/Dyrk1B in cancer. *Journal of cellular biochemistry* **102**, 274-279
38. Dabholkar, M., Vionnet, J., Bostick-Bruton, F., Yu, J. J., and Reed, E. (1994) Messenger RNA levels of XPAC and ERCC1 in ovarian cancer tissue correlate with response to platinum-based chemotherapy. *The Journal of clinical investigation* **94**, 703-708
39. Edwards, S. L., Brough, R., Lord, C. J., Natrajan, R., Vatcheva, R., Levine, D. A., Boyd, J., Reis-Filho, J. S., and Ashworth, A. (2008) Resistance to therapy caused by intragenic deletion in BRCA2. *Nature* **451**, 1111-1115
40. Sakai, W., Swisher, E. M., Karlan, B. Y., Agarwal, M. K., Higgins, J., Friedman, C., Villegas, E., Jacquemont, C., Farrugia, D. J., Couch, F. J., Urban, N., and Taniguchi, T. (2008) Secondary mutations as a mechanism of cisplatin resistance in BRCA2-mutated cancers. *Nature* **451**, 1116-1120

41. Haring, S. J., Mason, A. C., Binz, S. K., and Wold, M. S. (2008) Cellular functions of human RPA1. Multiple roles of domains in replication, repair, and checkpoints. *The Journal of biological chemistry* **283**, 19095-19111
42. Bastin-Shanower, S. A., and Brill, S. J. (2001) Functional analysis of the four DNA binding domains of replication protein A. The role of RPA2 in ssDNA binding. *The Journal of biological chemistry* **276**, 36446-36453
43. Bochkareva, E., Korolev, S., Lees-Miller, S. P., and Bochkarev, A. (2002) Structure of the RPA trimerization core and its role in the multistep DNA-binding mechanism of RPA. *The EMBO journal* **21**, 1855-1863
44. Fanning, E., Klimovich, V., and Nager, A. R. (2006) A dynamic model for replication protein A (RPA) function in DNA processing pathways. *Nucleic acids research* **34**, 4126-4137
45. Brosey, C. A., Yan, C., Tsutakawa, S. E., Heller, W. T., Rambo, R. P., Tainer, J. A., Ivanov, I., and Chazin, W. J. (2013) A new structural framework for integrating replication protein A into DNA processing machinery. *Nucleic acids research* **41**, 2313-2327
46. Fan, J., and Pavletich, N. P. (2012) Structure and conformational change of a replication protein A heterotrimer bound to ssDNA. *Genes & development* **26**, 2337-2347
47. Nuss, J. E., Sweeney, D. J., and Alter, G. M. (2009) Prediction of and experimental support for the three-dimensional structure of replication protein A. *Biochemistry* **48**, 7892-7905
48. Chen, H., Lisby, M., and Symington, L. S. (2013) RPA coordinates DNA end resection and prevents formation of DNA hairpins. *Molecular cell* **50**, 589-600
49. Li, X., and Heyer, W. D. (2008) Homologous recombination in DNA repair and DNA damage tolerance. *Cell research* **18**, 99-113
50. Sleeth, K. M., Sorensen, C. S., Issaeva, N., Dziegielewski, J., Bartek, J., and Helleday, T. (2007) RPA mediates recombination repair during replication stress and is displaced from DNA by checkpoint signalling in human cells. *Journal of molecular biology* **373**, 38-47
51. de Laat, W. L., Jaspers, N. G., and Hoeijmakers, J. H. (1999) Molecular mechanism of nucleotide excision repair. *Genes & development* **13**, 768-785
52. Araujo, S. J., Tirode, F., Coin, F., Pospiech, H., Syvaoja, J. E., Stucki, M., Hubscher, U., Egly, J. M., and Wood, R. D. (2000) Nucleotide excision repair of DNA with recombinant human proteins: definition of the minimal set of factors, active forms of TFIIH, and modulation by CAK. *Genes & development* **14**, 349-359
53. Hass, C. S., Lam, K., and Wold, M. S. (2012) Repair-specific functions of replication protein A. *The Journal of biological chemistry* **287**, 3908-3918
54. Lindsey-Boltz, L. A., Reardon, J. T., Wold, M. S., and Sancar, A. (2012) In vitro analysis of the role of replication protein A (RPA) and RPA phosphorylation in ATR-mediated checkpoint signaling. *The Journal of biological chemistry* **287**, 36123-36131

55. Anciano Granadillo, V. J., Earley, J. N., Shuck, S. C., Georgiadis, M. M., Fitch, R. W., and Turchi, J. J. (2010) Targeting the OB-Folds of Replication Protein A with Small Molecules. *Journal of nucleic acids* **2010**, 304035
56. Neher, T. M., Bodenmiller, D., Fitch, R. W., Jalal, S. I., and Turchi, J. J. (2011) Novel irreversible small molecule inhibitors of replication protein A display single-agent activity and synergize with cisplatin. *Molecular cancer therapeutics* **10**, 1796-1806
57. Neher, T. M., Shuck, S. C., Liu, J. Y., Zhang, J. T., and Turchi, J. J. (2010) Identification of novel small molecule inhibitors of the XPA protein using in silico based screening. *ACS chemical biology* **5**, 953-965
58. Shuck, S. C., and Turchi, J. J. (2010) Targeted inhibition of Replication Protein A reveals cytotoxic activity, synergy with chemotherapeutic DNA-damaging agents, and insight into cellular function. *Cancer research* **70**, 3189-3198
59. Chou, T. C. (2010) Drug combination studies and their synergy quantification using the Chou-Talalay method. *Cancer research* **70**, 440-446
60. Chou, T. C., and Talalay, P. (1984) Quantitative analysis of dose-effect relationships: the combined effects of multiple drugs or enzyme inhibitors. *Advances in enzyme regulation* **22**, 27-55
61. Herbert, M. R., Siegel, D. L., Staszewski, L., Cayanan, C., Banerjee, U., Dhamija, S., Anderson, J., Fan, A., Wang, L., Rix, P., Shiau, A. K., Rao, T. S., Noble, S. A., Heyman, R. A., Bischoff, E., Guha, M., Kabakibi, A., and Pinkerton, A. B. (2010) Synthesis and SAR of 2-aryl-3-aminomethylquinolines as agonists of the bile acid receptor TGR5. *Bioorganic & medicinal chemistry letters* **20**, 5718-5721
62. Chen, R., and Wold, M. S. (2014) Replication protein A: Single-stranded DNA's first responder: Dynamic DNA-interactions allow replication protein A to direct single-strand DNA intermediates into different pathways for synthesis or repair. *BioEssays : news and reviews in molecular, cellular and developmental biology*
63. Hamilton, T. C., Young, R. C., and Ozols, R. F. (1984) Experimental model systems of ovarian cancer: applications to the design and evaluation of new treatment approaches. *Seminars in oncology* **11**, 285-298
64. Hass, C. S., Gakhar, L., and Wold, M. S. (2010) Functional characterization of a cancer causing mutation in human replication protein A. *Molecular cancer research : MCR* **8**, 1017-1026
65. Givalos, N., Gakiopoulou, H., Skliri, M., Bousboukea, K., Konstantinidou, A. E., Korkolopoulou, P., Lelouda, M., Kouraklis, G., Patsouris, E., and Karatzas, G. (2007) Replication protein A is an independent prognostic indicator with potential therapeutic implications in colon cancer. *Modern pathology : an official journal of the United States and Canadian Academy of Pathology, Inc* **20**, 159-166
66. Storr, S. J., Chakrabarti, J., Barnes, A., Murray, A., Chapman, C. J., and Robertson, J. F. (2006) Use of autoantibodies in breast cancer screening and diagnosis. *Expert review of anticancer therapy* **6**, 1215-1223

67. Tomkiel, J. E., Alansari, H., Tang, N., Virgin, J. B., Yang, X., VandeVord, P., Karvonen, R. L., Granda, J. L., Kraut, M. J., Ensley, J. F., and Fernandez-Madrid, F. (2002) Autoimmunity to the M(r) 32,000 subunit of replication protein A in breast cancer. *Clinical cancer research : an official journal of the American Association for Cancer Research* **8**, 752-758
68. Wong, J. M., Ionescu, D., and Ingles, C. J. (2003) Interaction between BRCA2 and replication protein A is compromised by a cancer-predisposing mutation in BRCA2. *Oncogene* **22**, 28-33
69. Johnson, S. W., Perez, R. P., Godwin, A. K., Yeung, A. T., Handel, L. M., Ozols, R. F., and Hamilton, T. C. (1994) Role of platinum-DNA adduct formation and removal in cisplatin resistance in human ovarian cancer cell lines. *Biochemical pharmacology* **47**, 689-697
70. Hande, K. R. (1998) Etoposide: four decades of development of a topoisomerase II inhibitor. *European journal of cancer* **34**, 1514-1521
71. Sinha, B. K., Haim, N., Dusre, L., Kerrigan, D., and Pommier, Y. (1988) DNA strand breaks produced by etoposide (VP-16,213) in sensitive and resistant human breast tumor cells: implications for the mechanism of action. *Cancer research* **48**, 5096-5100
72. Choi, J. H., Gaddameedhi, S., Kim, S. Y., Hu, J., Kemp, M. G., and Sancar, A. (2014) Highly specific and sensitive method for measuring nucleotide excision repair kinetics of ultraviolet photoproducts in human cells. *Nucleic acids research* **42**, e29

Curriculum Vitae

Akaash K Mishra

Education

Indiana University, Indianapolis 2011-2014

- M.S., Biochemistry and Molecular Biology

Jaypee Institute of Information Technology, Noida 2006-2011

- Dual Degree B.Tech-M.Tech Biotechnology

Research Experience

Indiana University School of Medicine, Indianapolis

M.S. Research

Advisor: John Turchi, Ph.D.

Project: Developing small molecule inhibitors targeting replication protein A for platinum-based combination therapy.

- Results: Chemical inhibitor targeting the replication protein A-DNA interaction increases the efficacy of platinum-based chemotherapy in lung and ovarian cancer.

Publications

M. Akaash *et. al.,* Chemical inhibitor targeting the Replication Protein A-DNA interaction increases the efficacy of Pt-based chemotherapy in lung and ovarian cancer. [*In press,* Biochemical Pharmacology, 2014]

M. Akaash *et. al.,* CHIKVPRO – a protein sequence annotation database for Chikungunya Virus. Bioinformation 5(1): 4-6 (2010)

M. Akaash *et. al.,* High GC content: Critical parameter for predicting stress regulated miRNAs in Arabidopsis thaliana. Bioinformation 4(4): 151-154 (2009)